Cell and gene therapy via human neural stem/progenitor cells in the lithium-pilocarpine model of rat temporal lobe epilepsy

Haejin Lee

Department of Medical Science

The Graduate School, Yonsei University

Cell and gene therapy via human neural stem/progenitor cells in the lithium-pilocarpine model of rat temporal lobe epilepsy

Directed by Professor Kook In Park

The Doctoral Dissertation
submitted to the Department of Medical Science,
the Graduate School of Yonsei University
in partial fulfillment of the requirements for the
degree of Doctor of Philosophy

Haejin Lee

June 2015

This certifies that the Doctoral Dissertation of Haejin Lee is approved.

_____

Thesis Supervisor: Kook In Park

_____

Thesis Committee Member#1: Joon Soo Lee

_____

Thesis Committee Member#2: Won-Joo Kim

_____

Thesis Committee Member#3: Hyun Ok Kim

_____

Thesis Committee Member#4: Dong-Wook Kim

The Graduate School

Yonsei University

June 2015

ACKNOWLEDGEMENTS

I especially wish to express my sincere gratitude to my supervisor, Prof. Kook In Park, who has given me help, guidance, and encouragement throughout my doctoral program and made this dissertation possible.

I would also like to record my appreciation to Prof. Joon Soo Lee, Prof. Won-Joo Kim, Prof. Hyun Ok Kim, and Prof. Dong-Wook Kim for their valuable suggestions and comments on this dissertation.

Thanks are also due to lab colleagues for their assistance and useful suggestions in preparing this manuscript.

As always, my family has been there, providing all sorts of tangible and intangible support.

TABLE OF CONTENTS

LIST OF FIGURES

LIST OF TABLES

ABSTRACT

Cell and gene therapy via human neural stem/progenitor cells in the lithium-pilocarpine model of rat temporal lobe epilepsy

Haejin Lee

Department of Medical Science
The Graduate School, Yonsei University

(Directed by Professor Kook In Park)

Temporal lobe epilepsy (TLE), the most common and intractable type of adult focal epilepsy, is typically associated with pathological alterations in the hippocampus and parahippocampal regions. TLE is an attractive target for cell therapy due to its focal nature and associated cellular defects. Neural stem/progenitor cells (NSPCs) can continuously self-renew and give rise to intermediate and mature cells of both neuronal and glial lineages. Following transplantation in the diseased brain, NSPCs exhibit the potential to migrate toward the lesion and replace degenerated or ablated cells, as well as deliver therapeutic substances.

In this study, we transplanted human NSPCs (hNSPCs), derived from an aborted fetal telencephalon at 13 weeks of gestation and expanded in culture as neurospheres over a long time period, into the lateral ventricles of lithium-pilocarpine induced epileptic rats. Implanted hNSPCs migrated and integrated into the recipient brain. The majority of hNSPCs remained undifferentiated, although subsets of donor-derived cells differentiated into all three neural cell types of the central nervous system and expressed inhibitory neurotransmitter gamma-aminobutyric acid (GABA). We found that hNSPC transplantation

significantly reduced the frequency and duration of spontaneous recurrent motor seizures (SRMS) at 2 and 3 months post-transplants. In addition, hNSPC-transplanted epileptic rats showed neuroprotection, restoration of astrocytic glial cell-derived neurotrophic factor (GDNF) expression, and up-regulation of anti-inflammatory cytokines in the hippocampus. Finally, we demonstrated that conditioned medium from hNSPCs has neuroprotective action in an *in vitro* model of glutamate excitotoxicity. These results suggest that hNSPC transplantation possesses a therapeutic potential for treating TLE.

Next, we assessed the therapeutic efficacy of combined hNSPC and gene therapy in TLE. hNSPCs were engineered to secrete anticonvulsant neuropeptide galanin (GAL-hNSPCs) via adenoviral transduction. GAL-hNSPCs and green fluorescent protein (GFP)-expressing hNSPCs (GFP-hNSPCs) were transplanted into the hippocampus of lithium-pilocarpine induced epileptic rats. Transplanted both cell types migrated and dispersed throughout the hippocampus, and differentiated into TUJ1-, GFAP-, OLIG2-, and GABA-expressing cells. GFP-hNSPC transplantation significantly reduced the frequency and duration of SRMS at 3 months post-transplants, while GAL-hNSPC transplantation significantly reduced SRMS through all the time periods for 3 months following implantation. Moreover, GAL-hNSPC transplantation reversed the decreased anxiety seen in epileptic rats. GFP-hNSPC or GAL-hNSPC transplantation ameliorated neuronal loss, suppressed mossy fiber sprouting, and restored astrocytic GDNF expression in the hippocampus. GAL-hNSPC transplantation enhanced neuroprotection and reversed the declined neurogenesis. These results suggest that GAL-hNSPC transplantation represents a novel combined stem cell and gene therapy for suppressing seizures and rescuing emotional deficit in severely epileptic rats.

Key words: temporal lobe epilepsy, human neural stem/progenitor cells, lithium-pilocarpine, transplantation, cell therapy, gene therapy, galanin

Cell and gene therapy via human neural stem/progenitor cells in the lithium-pilocarpine model of rat temporal lobe epilepsy

Haejin Lee

Department of Medical Science
The Graduate School, Yonsei University

(Directed by Professor Kook In Park)

I. INTRODUCTION

Epilepsy is a chronic neurological disorder affecting tens of millions of people worldwide, and more than 30% of patients with epilepsy still have uncontrolled seizures despite conventional antiepileptic drugs (AEDs).[1] Temporal lobe epilepsy (TLE) is the most frequent and pharmaco-resistant type of adult focal epilepsy that presents with complex partial seizures, originating mainly from the mesial temporal structures such as the hippocampus or amygdala.[2,3] The rat lithium-pilocarpine model of epilepsy reproduces most clinical and neuropathologic features of human TLE.[4-6] In adult rats, the systemic injection of lithium and pilocarpine induces to status epilepticus (SE) followed by a latent period corresponding to epileptogenesis, and the occurrence of spontaneous recurrent seizures (SRS) which is accompanied by neuronal loss, mossy fiber sprouting (MFS), gliosis, abnormal neurogenesis, and inflammatory processes in the hippocampus.[6-11] Although surgical removal of epileptic foci is a recommended treatment for patients with TLE, this therapeutic option can lead to undesirable complications, such as significant cognitive impairment and lasting

dependence on AEDs.[12] For this reason, a continuing need exists for novel approaches that effectively control seizures in chronic TLE.

Stem cell-based cell transplantation has been investigated intensively for epilepsy treatment in various animal studies, although none of these approaches has yet been tested clinically in patients with epilepsy.[13-15] Over the past few years, embryonic stem cell (ES)-, neural stem cell (NSC)-, mononuclear bone marrow cell (BMC)-, or neural precursor-based approaches have been examined in animal models of epilepsy: mouse ES-derived neural precursors in pilocarpine- or kainic acid (KA)-induced status epilepticus (SE) or kindling-based TLE models,[16-19] rat fetal ganglionic eminence (GE)-derived neural precursors or NSC in the KA-induced TLE model,[10,20] mouse BMC in lithium-pilocarpine- or pilocarpine-alone-treated adult TLE model,[21,22] mouse fetal neural precursors from the medial ganglionic eminence (MGE) in congenital general epilepsy or pilocarpine-induced adult TLE models,[23,24] and immortalized human fetal brain-derived NSC in the pilocarpine-induced SE model.[25] These studies have demonstrated that neural stem/progenitor cell (NSPC)-based therapies in acute and chronic models of epilepsy exert anticonvulsant and antiepileptogenic effects, and replace degenerated or ablated neurons, repair damaged neural circuitry, and modulate neurotrophic expression. However, prior to the clinical application of NSPCs for epilepsy treatment, many challenges still must be addressed. It is essential to study human NSPCs (hNSPCs) derived from various cell sources, such as developing and adult brain tissues, ES, and induced pluripotent stem cells (iPSCs), for their abilities in terms of engraftment, migration, differentiation into specific neuronal or glial cells, seizure control, and functional recovery following transplantation into the brains of TLE models.[26]

A study demonstrated that substantial reductions in spontaneous recurrent motor seizures (SRMS) were observed for a short-term period after immortalized human fetal NSPCs were infused into the tail vein of the

animals a day following pilocarpine-induced SE.[25] However, that study was not pertinent for treating patients with TLE.

Because patients with epilepsy refractory to AED treatment are much in need of novel seizure-suppressing therapy, it is significant to examine the effects of hNSPC transplantation in animals with established epilepsy at the time of grafting. Previously, we cultivated and expanded several types of hNSPCs that were isolated from different brain regions of an aborted fetus at 13 weeks of gestation as neurospheres in culture dishes.[27] Among them, telencephalon-derived hNSPCs gave rise to not only neuronal and glial cells, but also differentiated into GABA-expressing cells *in vitro*. Additionally, other studies have demonstrated that intraventricular injection of NSPCs have several advantages, including wide distribution of grafted cells, less invasive delivery, injection of more cells, and easy application compared to intercerebral approach in the injured and degenerating CNS.[28-32] Lesions induced by pilocarpine represent multifocal brain damage,[5,33] which could require widespread distribution of grafted cells beyond the scope of conventional surgical procedures.

Given this background, we first investigated whether epileptic phenotypes could be improved in lithium-pilocarpine-induced TLE models by human fetal brain-derived NSPC transplantation into the lateral ventricles (LV) after epileptic seizures emerged, and characterized the distribution, engraftment, and the differentiation patterns of implanted cells in adult rat recipients.

Next, we assessed the therapeutic efficacy of combined hNSPC and gene therapy in TLE. Recently, neuropeptides, often termed endogenous anticonvulsant, have become a novel gene therapy target to treat focal epilepsy.[34] Galanin, a neuropeptide which acts as an inhibitory neuromodulator, is known to attenuate seizure activity in the hippocampus.[35-39] G-protein–coupled galanin receptor 1 (GALR1) and 2 (GALR2) are expressed in the hippocampus, play a role in the inhibition of epileptic

activity.[40] Mechanism of seizure suppression by galanin is thought to mediate through the closing of voltage-gated Ca^{2+} channels and/or the opening of ATP-sensitive K^{+} channels and ultimately pre-synaptic inhibition of gluamate transmission.[41-43]

Galanin injection into the hilus of hippocampus can attenuate seizure activity *in vivo*.[39] Adeno-associated virus (AAV)–mediated gene therapy with galanin has been described in animal models of TLE and acute seizures.[35,44,45] Infusion of a recombinant AAV to constitutively overexpress galanin into the rat dorsal hippocampus alleviated the number of seizure episodes and total time spent in seizure activity against intrahippocampal KA administration.[45] AAV vector carrying the fibronectin secretory signal sequence (FIB) preceding the coding sequence for the active galanin peptide (AAV-FIB-GAL) significantly attenuated *in vivo* focal seizure sensitivity and prevented KA-induced hilar cell death.[35] Another study demonstrated that encapsulation of galanin-producing cells was no need for direct genetic modification of the host cells via viral vector and immunosuppressant drugs, and the encapsulated galanin-producing cells showed a moderate anti-convulsant effect on focal seizures in kindling model of epilepsy.[36]

In contrast to encapsulated cells, which exert their therapeutic effect exclusively by paracrine action, stem cell-derived implants may survive long term, migrate, and integrate into the hippocampus[18] and may therefore directly influence the seizure activity. In the present study, we developed galanin-releasing hNSPC (GAL-hNSPC) using adenoviral vector carrying the Igκ leader secretory signal sequence preceding the coding sequence for the active galanin peptide under the control of the CAG promoter and green fluorescent protein (GFP) as a reporter, placed under IRES promoter control. To address the question whether GAL-hNSPCs combine hNSPCs and hNSPC-mediated galanin gene therapy, we investigated therapeutic effects on epileptic phenotypes in lithium-pilocarpine induced epileptic rats that received vehicle-

injection, GFP-expressing hNSPC (GFP-hNSPC) grafts, and GAL-hNSPC grafts into the hippocampus after epileptic seizures emerged.

II. MATERIALS AND METHODS

1. Cell culture

Human fetal brain tissue from a cadaver at 13 weeks of gestation was obtained with full parental written consent and approval of the Research Ethics Committee of Yonsei University College of Medicine, Seoul, Korea (Permit Number: 4-2003-0078).[46] In this study, hNSPCs for transplantation were derived from such a single donated fetal tissue. The culture of NSPCs was previously described in detail.[27] Briefly, after dissociation of telencephalic tissue in trypsin (0.1% for 30 min; Sigma, St. Louis, MO), cells were plated at 4 x 10^5 cells/mL in serum-free culture medium (DMEM/F12; Gibco, Grand Island, NY), N2 formulation (1% v/v; Gibco), and 8 μg/mL heparin (Sigma) supplemented with 20 ng/mL fibroblast growth factor-2 (FGF-2; R&D Systems, Minneapolis, MN) and 10 ng/mL leukemia inhibitory factor (LIF; Sigma). All cultures were maintained in a humidified incubator at 37°C and 5% CO_2 in air, and half of the growth medium was changed every 3–4 days. Proliferating single cells in culture generated free-floating neurospheres during the first 2–5 days of growth. They were passaged every 7–8 days by dissociation of bulk neurospheres with 0.05% trypsin/EDTA (T/E; Gibco).

For proliferation conditions, 8 × 10^5 cells/well were maintained with mitogens in 6-well plates for RT-PCR and Western blot. For differentiation conditions, neurospheres were trypsinized and dissociated into single cells, and cells were then placed on poly-L-lysine (PLL; 10 μg/mL; Sigma)-coated 8-well chamber slides (Nunc, Roskilde, Denmark) at 8 × 10^4 cells/well for immunocytochemical analysis or on PLL-coated 6-well plates (Sigma) at 1 × 10^6 cells/well for RT-PCR and Western blot in the growth medium without mitogens. The medium was replaced every 2 days, and cells were analyzed at

day 7 of differentiation.

2. Adenoviral vector construction and infection

We constructed recombinant adenoviral vectors carrying the Igκ leader secretory signal sequence preceding the coding sequence for the active galanin peptide under the control of the CAG promoter and GFP as a reporter, placed under IRES promoter control (Ad-Igκ-GAL-GFP). The Igκ leader secretory signal sequence was derived from pSecTag2 A (Invitrogen, Grand Island, NY). The coding sequence for the active human galanin was amplified by RT-PCR from 293A cell line RNA. The adenoviral vector that carried only IRES-GFP gene was used as a control (Ad-GFP). Adenoviral vectors were produced in conformity with the AdEasy^{TM} Adenoviral Vector System (Stratagene, La Jolla, CA, USA) manual. The infectious recombinant virus was purified by CsCl-gradient centrifugation and titrated on 293A cells by Tissue Culture Infecting Dose 50 (QBiogene, Carlsbad, CA, USA). Human NSPCs were infected by Ad-Igκ-GAL-GFP or Ad-GFP at a MOI of 0, 10, 20, 40, 80, 160, and 320 plaque-forming units per cell. The optimal MOI was determined from the transduction efficiency and cell viability. Flow cytometry confirmed that 95% of infected cells expressed GFP at the optimal MOI. The medium was replaced with fresh growth medium 10–12 hr after infection. GAL-hNSPCs and GFP-hNSPCs were incubated for 48 hr, and thereafter used for *in vivo* transplantation or *in vitro* studies. For proliferation conditions, 8×10^5 cells/well were maintained with mitogens in 6-well plates for RT-PCR. For differentiation conditions, neurospheres were trypsinized and dissociated into single cells, and cells were then placed on poly-L-lysine (PLL; 10 μg/mL; Sigma)-coated 8-well chamber slides (Nunc, Roskilde, Denmark) at 8×10^4 cells/well for immunocytochemical analysis or on PLL-coated 6-well plates (Sigma) at 1×10^6 cells/well for conventional RT-PCR or quantitative RT-

PCR in the growth medium without mitogens. The medium was replaced every 2 days, and cells were analyzed at day 7 of differentiation.

3. Characterization of galanin-releasing hNSPCs *in vitro*

Galanin secretion from GAL-hNSPCs and GFP-hNSPCs into culture medium was measured by a galanin ELISA kit according to the manufacturer's instructions (Peninsular Lab, LLC, San Carlos, CA, USA).

For CCK8 assay, 3×10^6 cells/well were maintained without mitogens in 6-well plate for 48hr, after which 50μl of CCK8 solution (Dojindo Laboratories Co., Kumamoto, Japan) was added to each well and the plate was incubated for 1–4 hrs. Cell viability was assessed by measuring absorbance at 450 nm using a microplate reader (Molecular devices, Menlo, CA, USA). Uninfected hNSPCs at the same passage served as controls.

To assess the proliferation rates of GAL-hNSPCs or GFP-hNSPCs, cells were plated onto 6-well plate at 8×10^5 cells/well and cultured without mitogen for 48hr and thereafter treated with EdU (5-ethynyl-2'-deoxyuridine; Invitrogen) at a final concentration of 200μM for 24 hr. Cells were fixed in 4% paraformaldehyde (PFA) in PBS, permeabilized with Perm/Wash™ buffer (BD Biosciences, San Diego, CA, USA) and stained with Alexa Fluor® 647 azide (Invitrogen). EdU-positive cells were quantified by flow cytometry.

For cell cycle analysis, cells were trypsinized and fixed in 75% ethanol overnight. Cells were washed with PBS and incubated with propidium iodide in FACS buffer (2% FBS in PBS) for at least 30min before flow cytometric analysis. Approximately 10,000 events were collected per sample and cell cycle data were modeled using FlowJo software (Miltenyi Biotec GmbH, Bergisch Gladbach, Germany).

Terminal dUTP nick end labeling (TUNEL) assay was performed using In Situ Cell Death Detection kit according to manufacturer's instruction (Roche

Applied Science, Indianapolis, IN, USA). Cells were fixed with 4% PFA in PBS for 1 hr at room temperature. The samples were washed with PBS and permeabilized by 0.1% Triton X-100 in 0.1% sodium citrate buffer for 15 min at 4 °C. After 3 times washing, cells were resuspended in TUNEL reaction mixture, and incubated for 60 min at 37 °C. TUNEL-positive cells were quantified by flow cytometry.

4. Reverse transcription-polymerase chain reaction (RT-PCR)

Total RNA was isolated from cell cultures or hippocampal tissue samples using the TRI reagent (MRC, Inc., Cincinnati, OH) according to manufacturer's instructions, and 1 μg of RNA was reverse-transcribed into cDNA using an oligo$(dT)_{18}$ primer and Superscript III reverse transcriptase (Invitrogen). Then, 1 μL of cDNA was amplified using Go-Taq polymerase (Promega, Madison, WI) in a thermal cycler (Eppendorf, Happauge, NY) according to the manufacturer's instructions. Primers sequences for human growth factors were listed in Table 1. To detect transcript expression for human galanin, GALR1, GALR2, and GALR3 in cell culture, the following primer sequences were used: human galanin, sense 5'-AAGCTTGGCTGGACCCTGAACAG-3' and antisense 5'-ACGCGTTTAGCTGGTGAGGC-3'; GALR1, sense 5'-ATCTGCTTCTGCTATGCCAAG-3' and antisense 5'-CAGTGGGCGGTGATTCTGA-3'; GALR2, sense 5'-GTCAACCCCATCGTTTACGC-3' and antisense 5'-CTCGCTCATGTGCAACAGGT-3'; GALR3, sense 5'-TCTGATGGGGAGATGGCTGAT-3' and antisense 5'-AGGATGAACAGGTCCGTGGT-3', and glyceraldehyde 3-phosphate dehydrogenase (GAPDH), sense 5'-ACCACAGTCCATGCCATCAC-3' and antisense 5'-TCCACCACCCTGTTGCTGTA-3'. The expression of PCR

products was normalized relative to the expression of GAPDH. To confirm *in vivo* expression of galanin, we performed RT-PCR using primers specific for the Igκ (5'-CATATGGAGACAGACACACT-3') and GAL (5'-ACGCGTTTAGCTGGTGAGGC-3') sequences in hippocampus in all groups at 3 months after transplantation. PCR products were separated on a 1.5% agarose gel and stained with ethidium bromide. As no template control, the extracted RNA was amplified with PCR without prior reverse transcription.

Table 1. Sequences of primers used for RT-PCR

Gene	Forward sequence (5' → 3')	Reverse sequence (5' → 3')
BDNF	AACAATAAGGACGCAGACTT	TGCAGTCTTTTTGTCTGCCG
NTF3	TACGCGGAGCATAAGAGTCAC	GGCACACACACAGGACGTGTC
NTF4	CCTCCCCATCCTCCTCCTTTT	ACTCGCTGGTGCAGTTTCGCT
NGF	ATGTCCATGTTGTTCTACACT	AAGTCCAGATCCTGAGTGTCT
VEGF	CCATGGCAGAAGGAGGAGG	ATTGGATGGCAGTAGCTGCG
FGF2	GTGTGCTAACCGTACCTGGC	CTGGTGATTTCCTTGACCGG
GDNF	CTGACTTGGGTCTGGGCTATG	TTGTCACTCACCAGCCTTTCTATT

5. Immunocytochemistry

Cultured cells were fixed with 4% paraformaldehyde (PF) in PIPES buffer (Sigma), rinsed with phosphate-buffered saline (PBS) solution, blocked with 3% bovine serum albumin (Sigma), 10% normal horse serum, and 0.3% Triton X-100 (Sigma) in PBS. Cultures were incubated with following primary antibodies: anti-human specific nestin (anti-hNestin; 1:200; Chemicon), anti-glial fibrillary acidic protein (GFAP; 1:1,000; Dako, Glostrup, Denmark), anti-neuronal class β-tubulin III (TUJ1; 1:1,000, Covance, Princeton, NJ), anti-vimentin (1:80; Sigma), anti-NF M (neurofilament M, 1:1000; Millipore), anti-NF H (1:1000; Millipore), anti-NF L (1:1000; Millipore), anti-Pax6 (1:40; Developmental Studies Hybridoma Bank), anti-GLAST (1:100; Santa Cruz Biotechnology, Santa Cruz, CA), anti-GABA (1:500; Sigma), anti-platelet-derived growth factor receptor alpha (PDGFR-α; 1:100; Santa Cruz Biotechnology), anti-Olig2 (1:500; Millipore, Billerica, MA), anti-S100β (1:1000; Sigma), and anti-GFP (1:200; Invitrogen). Species-specific secondary antibodies, conjugated with fluorescein (FITC; 1:180; Vector, Burlingame, CA) or Texas Red (TR; 1:180; Vector) were used to detect the binding of primary antibodies. Specimens were mounted using Vectashield mounting medium with 4,6-diamino-2-phenylindole (DAPI; Vector), and were analyzed by an immunofluorescence microscopy (BX51; Olympus, Center Valley, PA). For *in vitro* quantification, percentages of $hNestin^+$-, $TUJ1^+$-, $GABA^+$-, $GFAP^+$-, $S100\beta^+$-, and $OLIG2^+$ cells among total GFP^+ cells were calculated in three to five randomly selected fields. This sampling was replicated three times.

6. Induction of status epilepticus by lithium-pilocarpine

Adult male Sprague–Dawley (SD) rats (200–220 g) were kept on a 12/12-h

light/dark cycle (lights on at 07:00 h) with free access to food and water. This study was performed in strict accordance with the recommendations in the Guide for the Care and Use of Laboratory Animals of the National Institute of Health. The protocol was approved by the Committee on the Ethics of Animal Experiments of Yonsei University College of Medicine (Permit Number: 2013-0423).

Rats were infused with lithium chloride (127 mg/kg, i.p.; Sigma) 24 h prior to the administration of pilocarpine. On the next day, the rats were injected with methylscopolamine bromide (1 mg/kg, i.p.; Sigma) to limit the peripheral effects of pilocarpine, and 30 min later were injected with pilocarpine hydrochloride (45 mg/kg, i.p.; Sigma) to induce SE. Seizure events in pilocarpine-treated rats were scored according to the Racine[47]: Stage 1, facial movements only; Stage 2, facial movements and head nodding; Stage 3, facial movements, head nodding, and forelimb clonus; Stage 4, facial movements, head nodding, forelimb clonus, and rearing; Stage 5, facial movements, head nodding, forelimb clonus, rearing, and falling. Rats that did not develop stage 5 seizure were excluded from this study. Diazepam (Samjin, 10 mg/kg, i.p.) was injected 1 h after SE onset to cease seizure activity. The rats that went into SE were injected with 2.5 mL of 5% dextrose intraperitoneally twice a day and were given a moistened rat diet during the following 2–3 days. For 14–20 d after SE, pilocarpine-treated rats were monitored to confirm the emergence of SRMS by video recording. The frequency of SRMS (stages 3–5 seizure) was scored for 12 h/day.

7. Cell preparation and transplantation

Human NSPCs were maintained by passaging through the dissociation of bulk neurospheres and cryopreserved at each passage in the Good Manufacturing Practice facility. For transplantation, NSPCs taken at between

passage number 10 (P10) and P20 were selected and prepared. Cells were labeled with bromodeoxyuridine (BrdU; 3 μM; Sigma) for 5 days before grafts. At the time of grafting, cells were harvested by trypsinization after which the enzymatic activity was halted by soybean trypsin inhibitor (Sigma). The cells were centrifuged (900 × *g*, 3 min), the cell pellet was washed three times with H-H buffer, and the entire cell pellet was then resuspended in H-H buffer at a density of 1.0×10^5 cells/μL. The concentrated cells in a sterile freezing tube (Nunc) were then delivered to the animal operation room. For intracerebroventricular injection groups (vehicle and hNSPC groups), at 3 weeks after SE, epileptic rats were anesthetized and injected bilaterally into the lateral ventricle (ML ±2.1 mm, AP −1.2 mm, and DV −4.5 mm from bregma) with 7 μL/side of vehicle (H-H buffer only) or hNSPC suspension. For intrahippocampal injection groups (vehicle, GFP-hNSPCs, and GAL-hNSPC groups), at 3 weeks after SE, epileptic rats were anesthetized and injected into the CA3 regions of the bilateral hippocampi (ML ±4.2 mm, AP −4.52 mm, and DV −5.0 mm from bregma) with 4 μL/side of vehicle or cell suspension. Vehicle or cell suspension was infused at a flow rate of 1 μL/min using a 10-μL Hamilton syringe placed on an infusion pump (KD Scientific, Holliston, MA) controlled by a microprocessor. All animals in this study received daily injections of cyclosporine (10 mg/kg, i.p.) from a day before transplantation to the end of the experiment.

8. Monitoring of SRMS

The behavior of epileptic rats was observed at 1–3 months following transplantation to analyze the frequency, severity and duration of SRMS in both the vehicle-injected and NSPC-transplanted groups. Starting at 2 weeks following transplantation, the rats were video-monitored for 60 h per week (12 h/day, 5 days/week, 2 weeks/month, and 360 h in total). Rats were given

free access to water and food in individual cages and video-monitored during the daylight period. The video recordings were analyzed by observers blinded to group allocation. The frequency and severity of seizure, and the total time spent in seizure were assessed in each rat.

9. Morris water maze

The Morris water maze test was performed to assess learning and memory function in epileptic rats. The detailed method has been previously described.[48] Briefly, a circular polypropylene pool (200 cm in diameter and 40 cm in height) was filled with water (22 ± 1°C) made opaque with a food coloring agent, rendering it impossible for rats to see through it. On the pool rim, four points were designated (north, east, south, west), dividing the pool into four quadrants (NE, NW, SW, SE). A circular platform (15 cm in diameter and 30 cm in height) was positioned at the center of the SE quadrant and hidden 1 cm below the water surface, and the position of the platform was kept unchanged throughout the training days. A trial started when the rat was positioned in the water from a quasirandom start points and ended when the rat reached and escaped onto the hidden platform. The swim paths of rats were recorded by a video tracking system (SMART; Panlab, Barcelona, Spain) and analyzed thereafter. Rats were trained for 4 days, and the training day consisted of six trials with an interval of 5–15 min. If the rat was not able to find the platform in 120 s, the rat was guided to it by the investigator. Mean escape latency was calculated for each day during the training days. At the probe trial, on day 5, the rats were positioned in the opposite quadrant where the platform was previously located and allowed to swim in the pool without the platform for 60 s. All parameters of memory retention were measured. At the end of experiments, all rats were sacrificed by CO_2 inhalation as described above.

10. Injection scores

During each daily injection of the immunosuppressant cyclosporine the behavioral response of each rat to the injection was documented using a scale designed for assessment of the aggressiveness.[49] One point was given for each of the following reactions: (a) attempting to run away while being picked up from the cage, (b) urinating, (c) trying to escape while being held before the injection, (d) squirming, vocalizing, (e) attempting to push the syringe away or scratch the examiner, and (f) attempting to bite the examiner. Animals were tested twice a day, between 8 and 10 am and between 8 and 10 pm. Daily scores for each rat were obtained and the mean score for each rat was calculated monthly. The handler was same during the entire study, he was alone in the room during the injection time using the same handling technique; the environment for injections was maintained unchanged while the room kept quiet in order to minimize environmental sources of stress.[50]

11. Elevated plus maze

Anxiety-related behavior was evaluated using the elevated plus maze (EPM) as previously described.[5] The EPM apparatus was comprised of two open arms (50 × 12 cm) and two enclosed arms (50 × 12 × 40 cm), elevated 50cm above the floor level. Grip on the open arms is facilitated by inclusion of a small edge (0.5 cm high) around their perimeter. For testing, rats were brought to the room 1hr before the test and were tested individually. Before each trial, the maze was cleaned thoroughly with a 30% ethanol solution. At the beginning of the test, rats were placed in the central platform always facing the same open arm. The test lasted 5 min, and the behavior of each rat was recorded by a video tracking system (SMART; Panlab) and analyzed thereafter. Entries into an arm were defined when all four paws were in the

corresponding arm.[33] The time spent in the open arms was measured, with larger time in the open arms indicating lower levels of anxiety.

12. Immunohistochemistry

At the end of experiments, animals were deeply anesthetized with ketamine (75 mg/kg, i.p.) and xylazine (30 mg/kg, i.p.) and perfused with 4% PFA in 0.1M PIPES buffer. Brains were then removed, post-fixed, transferred in 30% sucrose in PBS for cryoprotection, and frozen in O.C.T compound (Sakura Finetek, Torrance, CA, USA). The brains were coronally sliced into 16-μm sections using a cryostat. Sections were washed in PBS and blocked with 3% bovine serum albumin (Sigma), 10% normal horse serum, and 0.3% Triton X-100 (Sigma) in PBS. Sections were incubated with following primary antibodies: anti-human specific nestin (anti-hNestin; 1:200; Chemicon), anti-human specific cytoplasm SC121 (1:500; Stem Cells, Inc., Cambridge, UK), anti-human specific GFAP SC123 (1:500; Stem Cells, Inc.), anti-glial fibrillary acidic protein (GFAP; 1:1,000; Dako), anti-neuronal class β-tubulin III (TUJ1; 1:500, Covance), anti-MAP2 (1:50; Cell signaling, MA, USA), anti-GABA (1:500; Sigma), anti-Olig2 (1:500; Millipore), anti-glial cell-derived neurotrophic factor (GDNF; 1:50; Santa Cruz Biotechnology), anti-S100β (1:1000; Sigma), anti-GFP (1:200; Invitrogen), anti-human specific nuclei (hNuc; 1:100; Chemicon), anti-NeuN (1:250; Chemicon), anti-parvalbumin (PV; 1:5000; Swant, Bellinzona, Switzerland), anti-zinc transporter 3 (ZnT3; 1:500; Synaptic Systems, Göttingen, Germany), anti-CD11b (1:100; Serotec, Oxford, UK), and anti-DCX (1:300; Santa Cruz Biotechnology) antibodies. Species-specific secondary antibodies, conjugated with fluorescein (FITC; 1:180; Vector, Burlingame, CA) or Texas Red (TR; 1:180; Vector) were used to detect the binding of primary antibodies. Specimens were mounted using Vectashield mounting medium with 4,6-

diamino-2-phenylindole (DAPI; Vector), and were analyzed by an immunofluorescence microscopy (BX51; Olympus, Center Valley, PA) or a confocal laser scanning microscopy (LSM 700; Carl Zeiss, Oberkochen, Germany). To determine differentiation patterns of grafted cells, sets of 50–100 $hNuc^+$ cells or GFP^+ cells from every fifth section were used to calculate the percentages of $hNestin^+$, $TUJ1^+$, $GFAP^+$, S100 β, $OLIG2^+$, or $GABA^+$ cells. At least 1000 cells per marker were analyzed.

13. Histological quantification

For quantification of neuronal damage, the density of $NeuN^+$ and PV^+ neurons was assessed manually at 400 × magnifications by an investigator unaware of the treatment group. Based on the data concerning neuronal damage induced by lithium-pilocarpine SE reported previously,[33,51,52] the examination of neuronal damage focused on pyramidal layer of the hippocampal CA3 (CA3ab and CA3c for assessment of $NeuN^+$ neuronal density) and CA1, and the hilus of the dentate gyrus. For each animal, every tenth brain sections containing the dorsal hippocampus were selected from bregma −3.1 to −3.6 mm. Neuronal densities were determined using the unbiased optical dissector technique as previously described.[53] Briefly, 3 counting frames (120 × 60 μm) were positioned in the CA1 and CA3 (3 for CA3ab and 2 for CA3c) of hippocampus and the entire hilus was used as the counting frame. The hilus was defined as the area bounded by the lower edge of the granule cell layer.[54] CA3c was defined as the CA3 pyramidal cell layer located between the blades of the dentate granule cell layer and CA3ab was defined as the CA3 pyramidal cell layer excluding the CA3 region.[55] CA1 was defined as the pyramidal cell layer that extended from the CA2 region to an imaginary line drawn perpendicular to the crest of the DG.[56] Neurons were identified as $NeuN^+$ and PV^+ cells that contained a relatively large (>8 μm)

soma to avoid counting glial cells. Neurons touching the inferior and right edge of the frame were not counted.

Mossy fiber sprouting was scored according to previously described.[57] A 1-in-15 series of brain sections sampled from the entire hippocampus was evaluated. Confocal optical sections of ZnT3 immunoreactivity in the dentate inner molecular layer were selected from the midpoint of the upper blade of the dentate at 630× magnifications (2024x2024 format). Optical sections were captured 2-3 μm below the tissue surface for all sections. For each section, mossy fiber sprouting was scored by first determining the area of the inner molecular layer present in the image, and then determining the percentage of the total area occupied by ZnT3 immnoreactive puncta using ImageJ software (NIH, Bethesda, MD, USA). Sensitivity was set to capture all puncta with an intensity >2X background and an area > 0.5μm.

For quantification of astrogliosis and microgliosis, confocal images of brain sections were collected at 400× magnifications in every fifteenth section through the dorsal hippocampus, and analyzed as previously described.[6] Briefly, images were transformed to 8-bit gray scale, and area fraction occupied by GFAP- or CD11b-immunoreactivity above threshold was obtained with the ImageJ software. The same threshold range was used in all images.

To investigate the level of GDNF expression in host hippocampal astrocytes, double immunofluorescence for GDNF and the astrocytic marker, S100β was performed, and $S100\beta^{+}$ astrocytes were visualized by Texas Red and GDNF expression was identified by fluorescein. The ratio of double-labeled GDNF- and S100β-positive cells among total S100β-positive cells in the DG, CA3, and CA1 of hippocampus was determined by a confocal laser scanning microscopy in every 10^{th} section throughout the dorsal hippocampus. At least 80 S100β-positive cells per animal were analyzed at 400× magnification.

To estimate the hippocampal neurogenesis, DCX^+ cells were counted in every fifteenth section through the entire hippocampus (from bregma –2.8 to –6.72 mm).[58] DCX^+ cells were counted at 40X magnification using a confocal microscopy. All DCX^+ cells in the granular cell layer (GCL), the subgranular cell layer (SGZ), and the hilus of dentate gyrus were counted per section by an observer blinded to group allocation. For cell counting, *z* stacks of 1-μm-thick single-plane images were captured through the entire thickness of the section. After images were collected per section, samples were stacked and analyzed using ImageJ software. Cell numbers were summed from all sections and multiplied by ten to obtain the total estimated number of cells per the GCL and the SGZ as previously published.[59]

14. Quantitative real-time reverse transcription-polymerase chain reaction (qRT-PCR)

Total RNA was isolated from cell cultures or hippocampal tissue samples using the TRI reagent (MRC, Inc., Cincinnati, OH), and 2 μg of RNA was reverse-transcribed into cDNA using random hexamer primers (Bioneer, Daejeon, Korea) and Superscript III reverse transcriptase (Invitrogen, Grand Island, NY) in a thermal cycler (Eppendorf, Happauge, NY) according to the manufacturer's instructions. Quantitative RT-PCR was carried out in a total volume of 10 μL containing 5 μL of LightCycler® 480 SYBR Green I Master (Roche Diagnostics Ltd., Rotkreuz, Switzerland), 0.5 μM of each primer and 2.5 μL of 1:10 diluted cDNA using LightCycler® 480 instrument (Roche Diagnostics Ltd). The cycling conditions were: 95° C for 5 min, followed by 45 cycles of 95°C for 10 s, 60°C for 10 s, and 72°C for 10 s. All the samples were carried out in triplicates. The expression levels of each mRNA expression were normalized to the housekeeping gene GAPDH using LightCycler® 480 Software, Version 1.5 (Roche Diagnostics Ltd). Primer

sequences for *NEUROG1* and *GAPDH* were retrieved from PrimerBank Database http://pga.mgh.harvard.edu/primerbank/.[60] Primers sequences for rat cytokines and chemokines were listed in Table 2.

Table 2. Sequences of primers used for qRT-PCR

Gene	Forward sequence (5' → 3')	Reverse sequence (5' → 3')
Il1b	AAGCCAAACAAGTGGTATTCTC	GATCCACACTCTCCAGCTGCA
Tnfa	TGTGCCTCAGCCTCTTCTCATTC	CATTTGGGAACTTCTCCTCCTTG
Il6	CCAGCCAGTTGCCTTCTTGGGA	TGGTCTGTTGTGGGTGGTATCCT
Il10	TAAGGGTTACTTGGGTTGCC	CTGTATCCAGAGGGTCTTCA
Il1rn	GCGCTTTACCTTCATCCGC	CTGGACAGGCAAGTGATTCGA
Il4	CAGGGTGCTTCGCAAATTTTAC	ACCGAGAACCCCAGACTTGTT
Ifng	AGTCTGAAGAACTATTTTAACT	CTGGCTCTCAAGTATTTTCGTGT
Cxcl8	CCCCCATGGTTCAGAAGATTG	TTGTCAGAAGCCAGCGTTCAC
Ccl5	GTCGTCTTTGTCACTCGAAGGA	GATGTATTCTTGAACCCACTTCT
Gapdh	TTGATTAAGTCCCTGCCCTTT	CGATCCGAGGGCCTAACTA

15. Multiplex immunoassay

Hippocampal tissue samples were weighed and homogenized in solution containing 50mM Tris-HCL (pH 7.6), 0.01% NP-40, 150mM NaCl, 2mM EDTA, 0.1% SDS, 1mM phenylmethylsulfonyl fluoride, and protease inhibitor cocktail (Sigma) at a ratio of 100μl solution to 10mg tissue. Samples were centrifuged at 4500 × g for 15min at 4°C, and then supernatants were collected and stored at −80°C. The concentrations of IL-1β, TNFα, IL-6, IL-10, IL-4, IFNγ, CXCL8, and CCL5 were determined using a Procarta Immunoassay kit (Affymetrix, Santa Clara, CA, USA) according to the manufacturer's protocol.

16. Hippocampal neuronal cell culture and experimental treatments

Dissociated cell culture were prepared from E18 SD rats based on previously described protocols.[61] At day 5 *in vitro* (DIV5), non-neuronal cell division was halted by addition of arabinose-C at a final concentration of 8μM and neurons containing <9% astrocytes, as determined by double immunostaining with MAP2 and GFAP, were used for experiments after DIV9. Cell conditioned medium was prepared by culturing hNSPCs ($1 \times 10^5/cm^2$) (hNSPC-CM) or human fibroblast IMR90 ($3 \times 10^4/cm^2$) (IMR90-CM) in Neurobasal medium with B27 supplement (NbB27; Gibco) for 3 days and used to replace 50% of the neuronal culture medium. Excitotoxicity was induced in DIV9 hippocampal neurons by exposure to 125μM glutamate (Sigma) for 15 min and measured using CCK8 assay (Dojindo).

17. Western blots

To assess differences in secreted growth factors between hNSPC-CM and

IMR90-CM, CM was concentrated 10-fold using Amicon Ultra-0.5 centrifugal filter devices (Millipore) in accordance with the manufacturer's guidelines. These concentrated CM were resolved by sodium dodecyl sulfate–polyacrylamide gel electrophoresis. Samples (20 μL) were loaded onto 10% Tris–glycine gels, and the proteins were transferred from the gel onto a 0.45-μm nitrocellulose membrane (Thermo Scientific, Suwanee, GA) over 4 h at 4°C. The protein blots were blocked with 5% skimmed milk in TBST and then incubated with 0.25% bovine serum albumin in TBST overnight at 4°C with the following primary antibodies: anti-BDNF (Santa Cruz Biotechnology), anti-NTF3 (Santa Cruz Biotechnology), anti-NTF4 (Santa Cruz Biotechnology), anti-NGF (Santa Cruz Biotechnology), and anti-VEGF (Santa Cruz Biotechnology). Immunoblots were rinsed with TBST, incubated with a horseradish peroxidase-conjugated secondary antibody (1:20,000; Jackson Immunoresearch, West Grove, PA) for 1 h at room temperature, and developed using SuperSignal West Pico Chemiluminescent substrate (1:20,000; Thermo Scientific). The images were scanned with a Fujifilm LAS-4000 mini imager and analyzed with the MultiGauge software (Fujifilm, Tokyo, Japan).

18. Statistical analysis

All data are shown as means ± standard error of the mean (SEM). Data were compared by Student's *t*-test, Mann–Whitney *U*-test, one-way analysis of variance (ANOVA) for multiple comparisons, nonparametric one-way ANOVA or repeated-measures ANOVA. All analyses were performed with SPSS 12.0 (SPSS Inc., Chicago, IL, USA). Differences were considered statistically significant for $P<0.05$.

III. RESULTS

1. Characterization of human NSPCs *in vitro*

Proliferating single cells isolated from the telencephalon of a human fetus at 13 weeks gestation (termed hNSPCs) gave rise to neurospheres that could be identified by their phase-bright appearance (Fig. 1A).[27] To identify the cellular composition of neurospheres, we assessed the expression of NSCs and the radial glial marker nestin,[62] and radial glial protein recognized by vimentin, GFAP, Pax6, and the glutamate astrocyte-specific transporter (GLAST or EAAT1).[63-68] Additionally, we analyzed expression levels of GFAP, a protein expressed by immature cells or astrocytes, neuron-specific β-tubulin III (TUJ1), and neuronal markers NF and NeuN. Most cells (95–99%) expressed vimentin, nestin, GFAP, TUJ1, and Pax6 (Fig. 1B, D, E, H, or J, respectively), while those labeled by the GLAST antibody were distributed exclusively in the outer regions of the spheres (Fig. 1M–O). More than 90% of GFAP-labeled cells co-expressed nestin, vimentin or Pax6, suggesting that these cells represent radial glia cells, which are recognized as multipotent NSPCs[67,69,70] (Fig. 1B, D–F, or J–L). In addition, more than 90% of $GFAP^+$ cells expressed the early neuronal marker TUJ1 at relatively low to moderate levels (Fig. 1G–I), suggesting that cells are double-labeled with glial and neuronal markers are multipotent progenitors.[68,71] Interestingly, some cells that strongly expressed TUJ1 were found predominantly in the sphere core and were not co-labeled with GFAP (Fig. 1H and I), indicating that even under proliferative conditions, some early neurons are generated in the spheres. However, these cells did not express mature neuronal markers, such as NF (Fig. 1C) or NeuN (data not shown). These data demonstrate that mutipotent NSCs, progenitors, and radial glial cells may co-exist with some restricted neuronal or glial progenitors in human neurospheres derived from

the fetal telencephalon.

Next, we performed immunostaining to explore the hNSPCs' ability to differentiate into three neural cell types *in vitro*: neurons, oligodendrocytes, and astrocytes (Fig. 2). Seven days after plating neurosphere-derived single cells under differentiation conditions, the hNSPCs had differentiated into $TUJ1^+$ neurons, $OLIG2^+$ oligodendrocyte progenitors, and $GFAP^+$ astrocytes (Fig. 2A–C), and approximately 17% of the hNSPCs co-expressed TUJ1 and GABA (Fig. 2D). Thus, the hNSPCs exhibited characteristics consistent with NSCs,[72-75] such as neurosphere formation, expression of neural stem/progenitor cell markers, and multipotent differentiation.

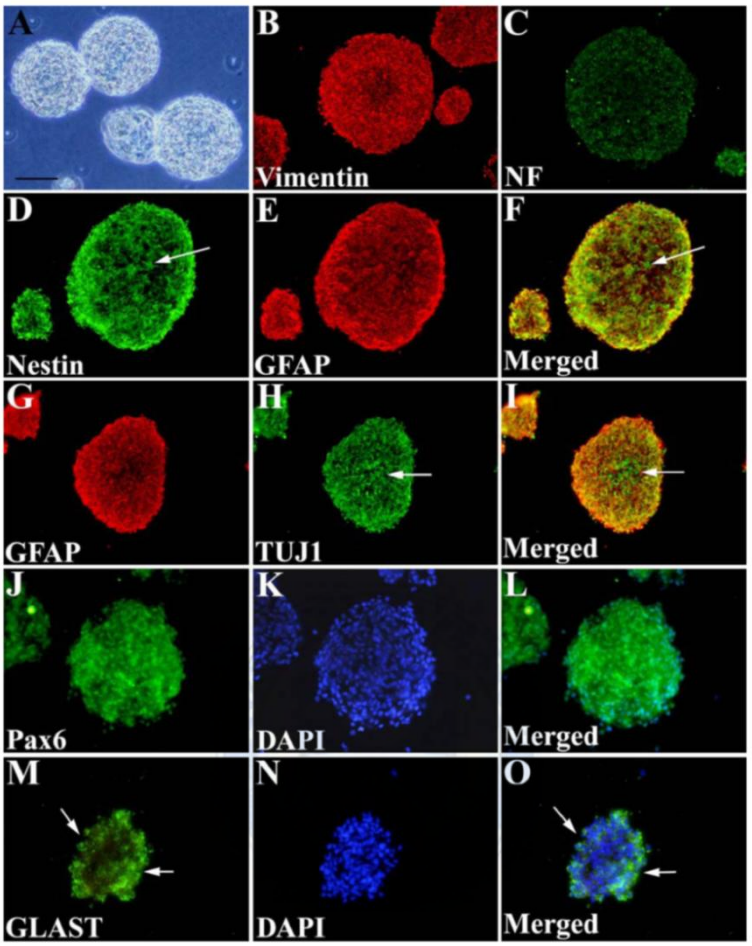

Figure 1. Neurosphere formation by fetal human CNS tissue and cellular composition of the neurosphere. Phase microscopy (A) and immunofluorescence labeling (B–O) of representative neurospheres grown in FGF-2 and LIF. The sectioned neurospheres were stained for vimentin (B), NF HML (C), nestin (D and F; green), GFAP (E, G and I; red), TUJ1 (H and I; green), Pax6 (J and L; green), GLAST (M and O; green), and DAPI (K, L, N, and O; blue). Note that the majority of the cells in the neurospheres express vimentin, nestin, GFAP, TUJ1, and Pax6 (B, D, E, H, and J, respectively), while GLAST staining appears in the outer portions of the spheres (arrows in

M and O). (D–F) More than 90% of the GFAP-expressing cells (E; red) co-express nestin (D; green), as observed under the dual-filter microscope (F; yellow or orange). A few cells within the neurospheres are labeled with the anti-nestin antibody and not with the anti-GFAP antibody (arrows in D and F; green). (G–I) More than 90% of the GFAP-expressing cells (G; red) co-express TUJ1 in relatively low to moderate levels (H; green), as observed under the dual-filter microscope (I; yellow or orange). Some cells that express TUJ1 at high levels, but that are not labeled with the anti-GFAP antibody, are located predominantly in the neurosphere core (arrows in H and I; green). Scale bar = 100μm.

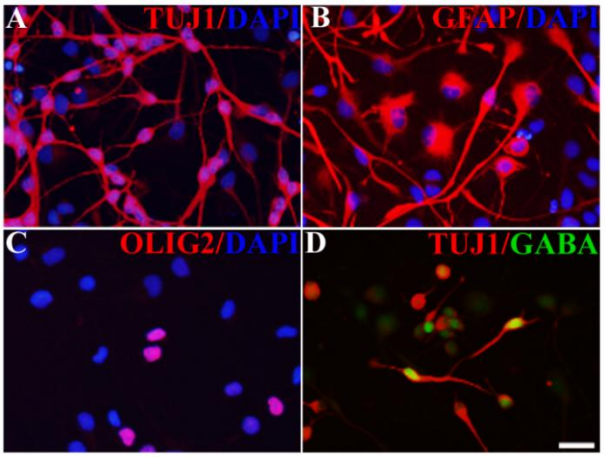

Figure 2. Multipotent hNSPCs and differentiation into GABAergic neurons in culture. (A–C) Under differentiation conditions, differentiation of fractions of hNSPCs into $TUJ1^+$ neurons visualized by Texas Red (A), $GFAP^+$ astrocytes imaged using Texas Red (B), and $OLIG2^+$ oligodendrocyte progenitors identified by Texas Red (C) could be observed. Nuclei were counterstained with DAPI. (D) Some hNSPC-derived differentiated neurons were co-labeled with TUJ1 (red) and GABA (green). Scale bar = 50 μm.

2. Engraftment and distribution of hNSPCs following transplantation

To evaluate the migration and engraftment patterns of hNSPCs in epileptic brain lesions, we injected hNSPCs into the LV of epileptic rats at 21 days after SE. Animals were sacrificed 3 months post-transplants, and brain tissues were processed for immunohistochemistry using hNuc or SC121 antibodies to detect human cells. The distribution of grafted hNSPCs is illustrated in Fig. 3A. Donor-derived cells were present in the LV (Fig. 3B), the subventricular zone (SVZ) (Fig. 3B and 4E), fimbria of the hippocampus (Fig. 3D), the corpus callosum (Fig. 3C), the neocortex (Fig. 3E), and the external capsule (Fig. 3F), indicating the robust engraftment, long-term survival, and extensive migration of grafted cells.

3. Differentiation of hNSPCs in epileptic rats following transplantation

We investigated differentiation patterns of donor-derived cells in the brains of epileptic rats at 3 months following transplantation (Fig. 4A–U). The majority of $hNuc^+$ cells expressed nestin (87.7% ± 9.4%), indicating that hNSPC-derived cells remained largely undifferentiated (Fig. 4A–D). Donor-derived cells also expressed the early neuronal marker TUJ1 (11.5% ± 2.4%; Fig. 4E–H), the immature cell and astrocyte marker GFAP (64.4% ± 11.0%; Fig. 4I–L), the oligodendrocyte progenitor marker OLIG2 (3.7% ± 1.9%; Fig. 4M–P), or GABA (7.2% ± 0.8%; Fig. 4Q–T). Because many $GFAP^+$ donor-derived cells expressed nestin, we identified these cells as immature cells, not mature astrocytes (data not shown). In addition, very few $hNuc^+$ cells co-expressed for the astrocyte marker S100β (<1%). These findings suggest the majority of hNSPCs grafted into LV of epileptic rats remain undifferentiated, although subsets of donor-derived cells express neuronal or glial lineage markers.

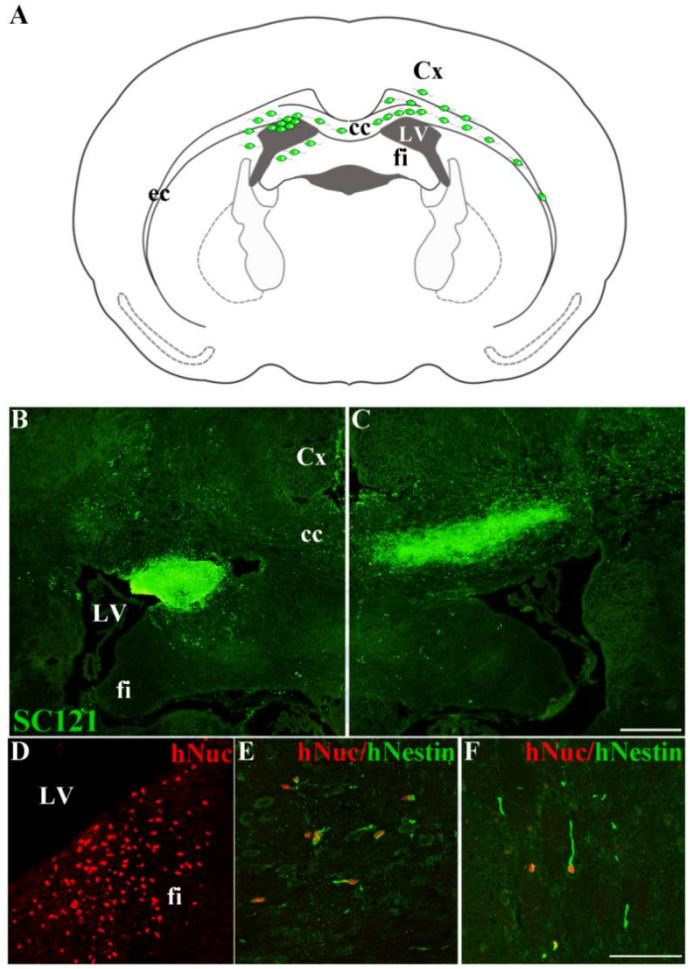

Figure 3. Engraftment and distribution of hNSPCs that grafted into the LV of epileptic rats. (A) A schematic figure illustrates the distributions of grafted cells in rats 3 months after transplantation. (B and C) $SC121^{+}$ grafted cells (green) were located in the LV, the SVZ, and fimbria of the hippocampus (B), and the corpus callosum (C). (D) Immunofluorscence staining with hNuc (red) showed that transplanted cells integrated into fimbria of the hippocampus. Double-immunostaining with hNuc (red) and hNestin (green) revealed the migration of grafted hNSPCs into the neocortex (E) and along external capsule (F). Scale bar=500 μm (B and C) and 100 μm (D–F).

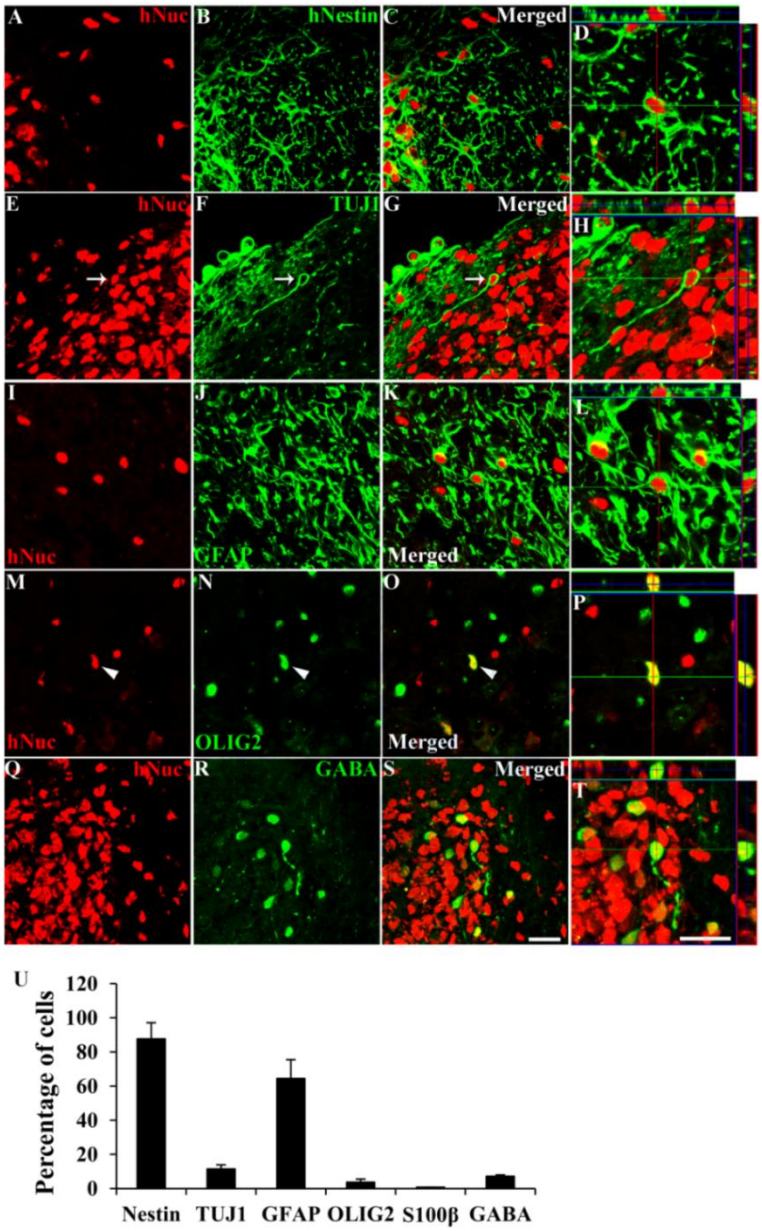

Figure 4. Differentiation of hNSPCs following transplantation into the LV of epileptic rats. (A–T) $hNuc^{+}$ grafted cells (red) were co-stained with nestin (green; A–D), TUJ1 (green, arrow in E–H), GFAP (green; I–L), OLIG2 (green, arrowhead in M–P), and GABA (Q–T). (D, H, L, P and T) Orthogonal view

from confocal *z*-series showed that hNuc (red) in nuclei and cell type-specific marker (green) in cytoplasm were expressed in the same cell. Scale bar=20 μm (S), 20 μm (T). Quantification of the data presented in (U).

4. Effect of hNSPC transplantation on SRMS and behavioral abnormalities

We examined whether hNSPC grafting could control spontaneous seizures in pilocarpine-treated rats over a long-term follow-up period. From 2 weeks to 3 months following transplantation, seizure activity was evaluated by video monitoring (12 h/day, 5 days/week, and 2 weeks/month for 360 h total). In hNSPC-grafted epileptic rats, SRMS frequencies were significantly reduced at 2 and 3 months after grafting (0.02 ± 0.01 and 0.07 ± 0.02 seizures/day, respectively), compared with vehicle-injected epileptic rats (0.14 ± 0.05 and 0.28 ± 0.07 seizures/day, respectively; Fig. 5A). The total time spent in SRMS was also reduced in hNSPC-grafted epileptic rats at 2 and 3 months after transplantation (4.23 ± 1.71 sec and 12 ± 3.63 sec, respectively) compared to that in vehicle-injected epileptic rats (23.38 ± 8.72 sec and 56.11 ± 18.79 sec, respectively; Fig. 5B). Seizure severity was usually stage 4 or 5 and did not differ significantly between vehicle-injected and hNSPC-transplanted rats (Fig. 5C).

Lithium-pilocarpine treated rats also exhibit behavioral deficits in spatial learning or aggressive response to injection,[25,76] thus we next examined whether hNSPC transplantation could reduce aggressive behavior via injection score test. The epileptic rats showed significantly higher injection scores, and therefore aggressiveness, compared to non-epileptic control rats (Fig. 5D) as found in previous studies.[25,77] Injection scores did not change significantly after hNSPC grafting ($P > 0.05$; Fig. 5D), indicating that hNSPC transplantation did not improve aggressiveness in the epileptic rats.

To evaluate the effect of hNSPC grafting on learning and memory function in the pilocarpine model, we conducted water maze testing at 3 months post-transplantation. In the hidden platform test, epileptic rats that received vehicle exhibited significantly longer escape latencies compared to non-epileptic control rats (Fig. 5E), indicating that these rats had a learning impairment.

This deficit was confirmed in the probe test (Fig. 5F–I), during which the epileptic rats in the vehicle group spent less time in the target quadrant and platform area (Fig. 5F, G), took longer to reach the platform area (Fig. 5H), and crossed the platform area in less time (Fig. 5I) when the platform was removed. The hNSPC-grafted rats did not show improvement in overall spatial learning or memory function, and were indistinguishable from the vehicle-injected group.

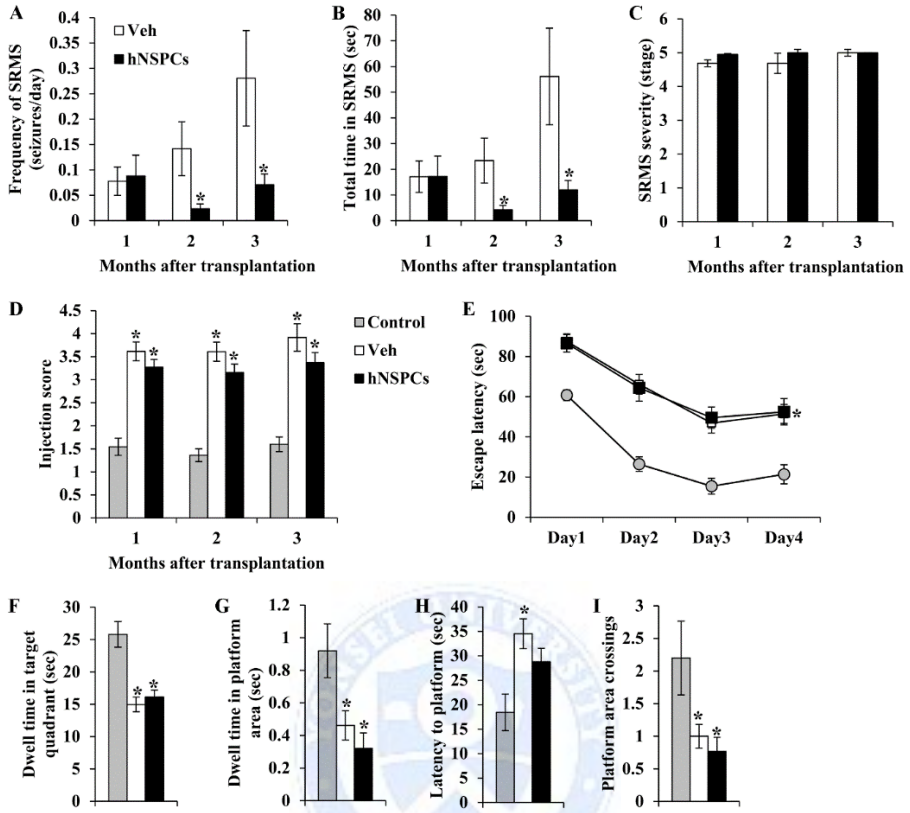

Figure 5. Effects of hNSPC grafting on SRMS, aggressiveness, spatial learning and memory function in epileptic rats. (A–C) Seizure activity was evaluated. The mean seizure frequencies (A), total time spent in seizures (B) and seizure stages (C) were calculated during 1, 2, and 3 months following transplantation in vehicle-injected and hNSPC-transplanted groups. * Significantly different from vehicle group at $P < 0.05$. (D) The behavioral response to the injection was documented to assess the aggressiveness during 1, 2, and 3 months following transplantation in control, vehicle-injected, and hNSPC-transplanted groups. * Significantly different from control at $P < 0.05$. (E–I) In a Morris water maze test, Escape latency decreased gradually and significantly over the 4 days of testing in control rats, but not in vehicle- and hNSPC-injected epileptic rats (E). During probe testing on day 5, dwell time

in the target quadrant (F), dwell time in the platform area (G), latency to the platform (H), and platform area crossings (I) were measured in the three groups. Both of vehicle- and hNSPC-injected epileptic rats exhibited significant deficits in memory retention in terms of all parameters. * Significantly different from control at $P < 0.05$; error bars indicate ± SEM.

5. Effect of hNSPC transplantation on histopathological changes in the hippocampus

To explain how hNSPC grafting suppress seizures in the rats, we analyzed the effects of cells treatment 3 months post-transplantation on histopathological alterations that resemble findings in human TLE patients, including neuronal damage, mossy fiber sprouting (MFS), astrogliosis, and microgliosis in the hippocampus. Immunohistochemical staining with anti-NeuN antibody showed that neuronal density in the pyramidal cell layers of CA3c, CA3ab, CA1 and in the hilus of the dentate gyrus (DG) were significantly reduced in vehicle-injected epileptic rats (Fig. 6A*b* and A*e*, $P < 0.01$), compared to non-epileptic control rats (Fig. 6A*a* and A*d*). Human NSPC grafting significantly ameliorated neuronal loss in CA3c (Fig. 6A*c* and A*f*) but did not improve neuronal loss in the hilus, CA3ab, or CA1 regions (Fig. 6C). Loss of parvalbumin $(PV)^+$ neurons in the hippocampus has been observed in epileptic rats[4,51,78], thus we also investigated whether hNSPC grafting affected the number of PV^+ neurons in hippocampal subfields, including the hilus, CA3, and CA1 regions. Compared to non-epileptic control rats, a significant loss of PV^+ neurons was detected in the hilus (42% cell loss), CA3 (33%), and CA1 (41%) regions in vehicle-injected epileptic rats (Fig. 6B and D, $P < 0.05$). In hNSPC-transplanted rats, the hilus showed a significant reduction of PV^+ neurons ($P < 0.05$), but CA3 and CA1 exhibited the significantly higher number of PV^+ neurons than those in vehicle-injected epileptic rats ($P = 0.09$ and $P = 0.001$, respectively). Taken together, the above data indicate hNSPC grafting leads to a substantial preservation of pyramidal neurons in CA3c and of PV^+ neurons in CA1. As a previous study demonstrated that a loss of PV^+ neurons is directly related to seizure severity[7], survival of PV^+ neurons in CA1 could play an important role in seizure suppression that is mediated by hNSPC transplantation.

Aberrant sprouting of granule cell axons (mossy fibers) into the inner molecular layer (IML) of the DG of the hippocampus is one of the best-known structural changes that occur in TLE models. [2,3,79,80] To visualize mossy fibers, we performed zinc transporter 3 (ZnT3)-specific immunostaining that selectively label mossy fiber terminals, and MFS was scored by measuring the total areas containing ZnT3 immunoreactive puncta in the DG IML, as previously described [57]. Robust MFS were observed in vehicle- and hNSPC-injected epileptic rats (% IML MFS = 10.8 ± 2.0 and 8.6 ± 2.0, respectively; Fig. 7B and C), but not in control rats (% IML MFS = 0.8 ± 0.0; Fig. 7A). The extent of MFS was not significantly different between vehicle- and hNSPC-injected rats ($P > 0.05$; Fig. 7D), indicating that the significant decrease in seizure frequency seen with hNSPC transplantation did not the result from a reversal of aberrant MFS in the DG.

We also analyzed astrogliosis and microgliosis in the hippocampal subfields such as the hilus of DG, CA3, and CA1 (Fig. 8). To assess astrogliosis, we conducted immunohistochemcal staining for GFAP and measured the area occupied by GFAP as previously described.[81,82] $GFAP^+$ astrocytes in both of vehicle- and hNSPC-injected epileptic rats showed a large cell body with thick cellular processes (Fig. 8B and C), while astrocytes of non-epileptic control rats exhibited normal morphologies (Fig. 8A). In the hilus, CA3, and CA1 regions, the average GFAP immunoreactive area had significantly increased in vehicle- and hNSPC-injected epileptic groups compared to the control rats, indicating reactive astrogliosis.[6] No significant difference was observed in reactive astrogliosis between vehicle- and hNSPC-injected epileptic rats (Fig. 8G). Immunohistochemical staining with anti-CD11b antibody revealed that activated microglia were present in the hippocampal subfields of vehicle-injected epileptic rats (Fig. 8E), but not in non-epileptic control rats (Fig. 8D). Similar to astrogliosis, the mean area occupied by $CD11b^+$ cells was significantly increased in vehicle-injected epileptic rats

compared to non-epileptic control rats (Fig. 8H). We observed more extensive microgliosis in especially CA1 region than in the hilus or CA3 region (Fig. 8H). There was no significant difference in microgliosis between vehicle- and hNSPC-injected rats (Fig. 8F). These results suggest that hNSPC grafting did not influence astrogliosis and microgliosis in the hippocampal subfields in epileptic rats.

6. Effect of hNSPC grafting on the expression of GDNF in host hippocampal astrocytes

Increased GDNF levels in hippocampal astrocytes of the epileptic brain suppress seizures.[83,84] According to Waldau et al., rat NSC grafting that added new donor-derived $GDNF^+$ cells and restored GDNF expression in host hippocampal astrocytes restrained SRMS in a TLE model.[10] However, we did not observe hNSPC-derived GDNF-expressing astrocytes in the hippocampus following transplantation, but hNSPC transplantation induced GDNF expression in the majority (74% for hilus, 68% for CA3, and 84% for CA1) of host hippocampal astrocytes in the epileptic rats (Fig. 9I–L). Levels of GDNF expression were mostly restored to level of the intact controls (Fig. 9A–D and F). In contrast, levels of GDNF expression of host astrocytes was 49% in hilus, 53% in CA3, and 63% in CA1 of vehicle-injected epileptic rats (Fig. 9E–H). Levels of GDNF expression were not restored to level of the intact controls by vehicle-injection(Fig. 9M). Thus, hNSPC transplantation induced GDNF expression in host hippocampal astrocytes which may be involved in suppressing seizures.

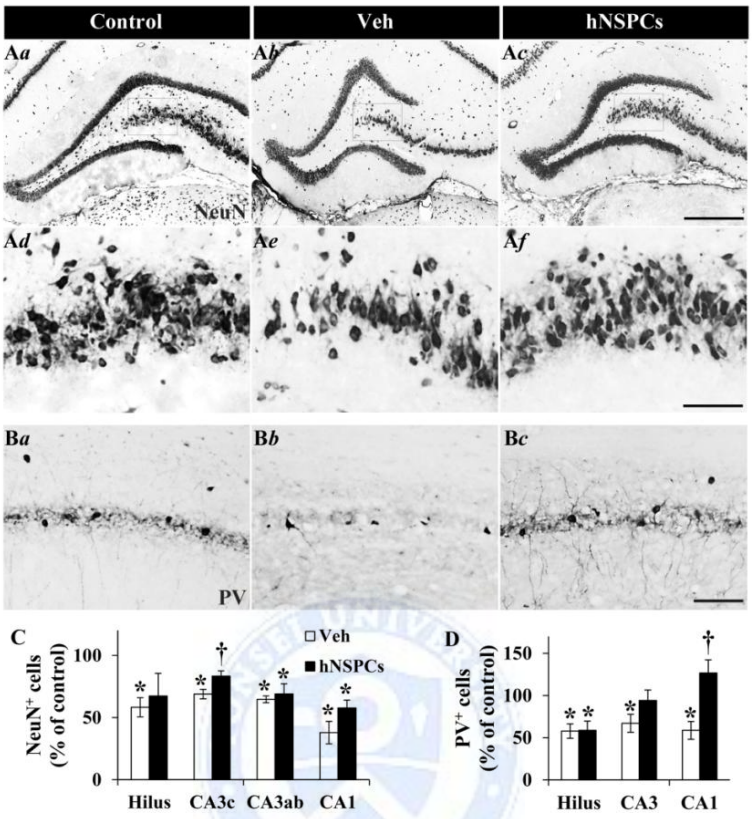

Figure 6. Effect of hNSPC transplantation on neuronal damage in the epileptic hippocampus. (A and C) hNSPC grafting significantly relieved $NeuN^+$ neuronal loss in the pyramidal cell layer of CA3c region. Representative NeuN stained sections of CA3c region of control rat (A*a* and A*d*), and epileptic rat that received vehicle injection (A*b* and A*e*) or hNSPC grafting (A*c* and A*f*). Boxed region in A*a*, A*b* and A*c* is magnified in A*d*, A*e* and A*f*, respectively. Scale bar=500 μm (A*c*), 100 μm (A*f*). (B and D) Human NSPC grafting led to a substantial preservation of PV^+ neurons in CA1. Representative staining for PV of CA1 region in control (B*a*), vehicle-injected (B*b*), and hNSPC-grafted (B*c*) groups. Scale bar=100 μm (B*c*). Bar graphs illustrated the percentage of remaining $NeuN^+$ neurons (C) and PV^+ neurons (D) in the hippocampal subfields. * Significantly different from control at $P <$

0.05; † significantly different from vehicle-injected group at $P < 0.05$; error bars indicate ± SEM.

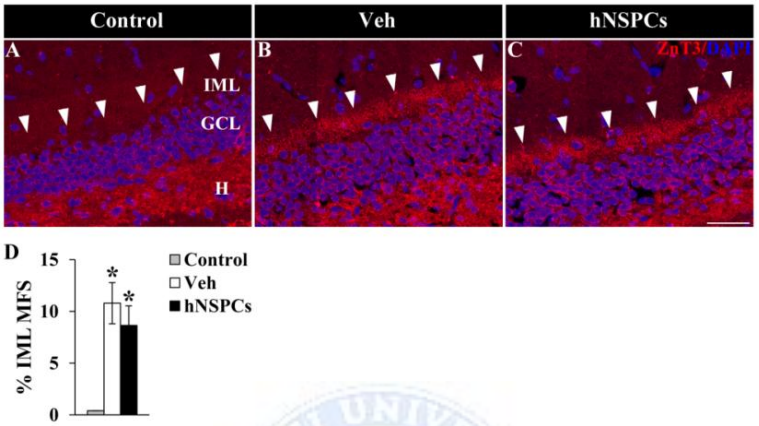

Figure 7. Effect of hNSPC transplantation on MFS in the epileptic hippocampus. Robust MFS were observed in vehicle-injected (B) and hNSPC-grafted epileptic rats (C) but not in control rats (A). Abbreviations: IML, inner molecular layer; GCL, granular cell layer; H, hilus. Scale bar=50 μm. (D) Quantification showed the extent of MFS was not significantly different between vehicle- and hNSPC-injected rats. * Significantly different from control at $P < 0.05$; error bars indicate ± SEM.

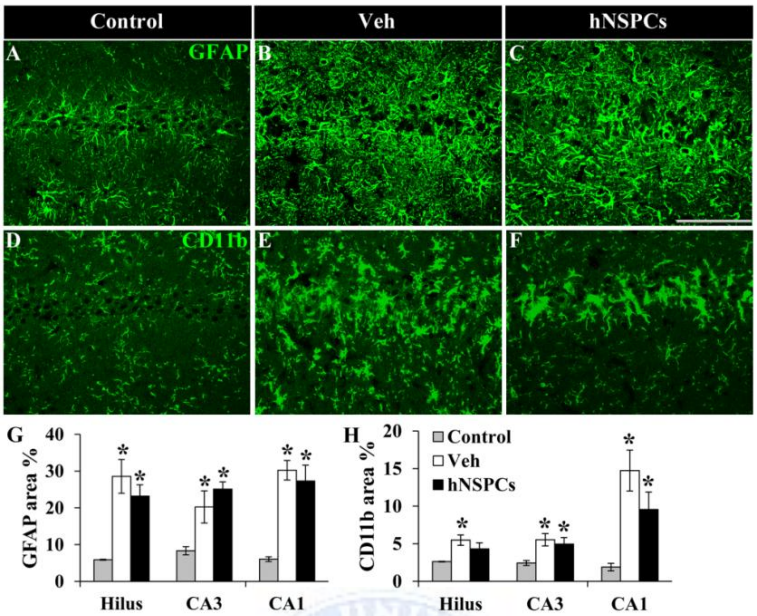

Figure 8. Effect of hNSPC transplantation on astrogliosis and microgliosis in the epileptic hippocampus. GFAP immunostaining showed that the GFAP immunoreactive area significantly increased in vehicle- (B) and hNSPC-injected groups (C) compared to the control rats (A), indicating reactive astrogliosis. (G) No significant difference was observed in reactive astrogliosis between vehicle- and hNSPC-injected epileptic rats. * Significantly different from the control at $P < 0.05$; error bars indicate ± SEM. (E–F) Immunostaining with CD11b revealed that activated microglia were present in the CA1 region of vehicle- (E) and hNSPC-injected (F) epileptic rats, but not in non-epileptic control rats (D). (H) Bar graphs illustrate the percentage of area occupied by $CD11b^{+}$ cells in the hippocampal subfields in the three groups. * Significantly different from the control at $P < 0.05$; error bars indicate ± SEM. Scale bar=100 μm.

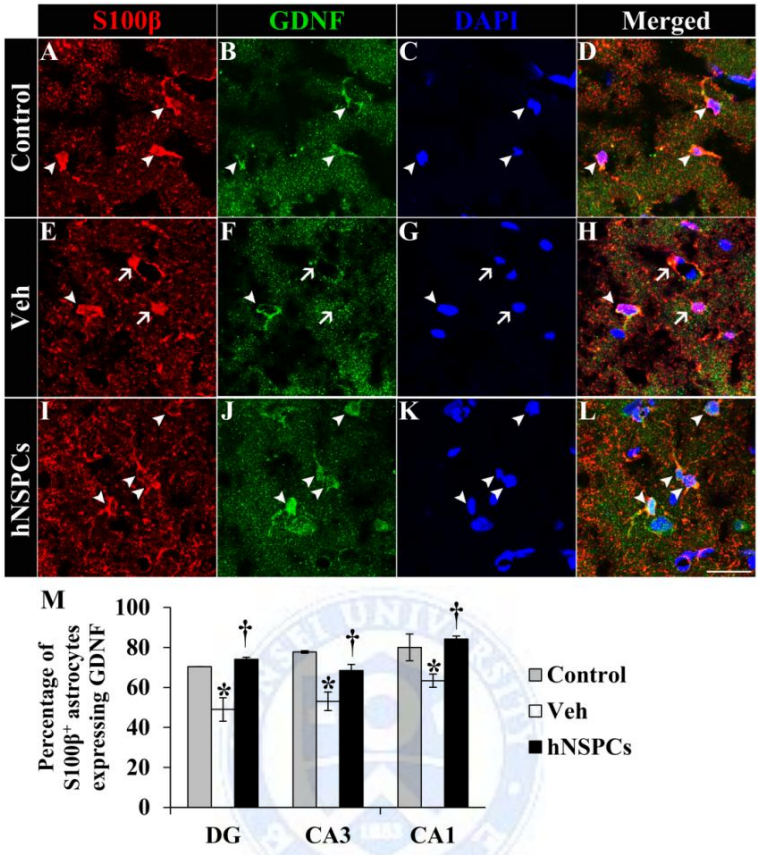

Figure 9. Effect of hNSPC grafting on the expression of GDNF in host hippocampal astrocytes. GDNF expression in S100β^{+} hippocampal astrocyte was observed in an age-matched intact control rats (A–D), vehicle- (E–H), and hNSPC-injected epileptic rats (I–L). Nuclei were counterstained with DAPI (C, G, and K). Arrowheads in A-L indicated S100β/GDNF double-labeled cells. Arrows in E, G and H denoted S100β^{+} host hippocampal astrocytes that were devoid of GDNF immunoreactivity in vehicle-injected epileptic rats. Scale bar=50 μm. (M) The bar chart represents percentages of S100β^{+} astrocytes expressing GDNF in the hippocampal subfields in the three groups. * Significantly different from the age-matched intact control group at $P < 0.05$; † significantly different from vehicle-injected group at $P < 0.05$; error bars indicate ± SEM.

7. Neuroprotective effect of hNSPCs against glutamate-induced excitotoxicity *in vitro*

As discussed above, hNSPC grafting promotes neuroprotection in hippocampal neurons while a few grafted cells differentiated into neurons in the hippocampus of recipient rat brain. Therefore, we wondered if soluble factors secreted by hNSPCs protected hippocampal neurons against glutamate-induced excitotoxicity. To study this paracrine hypothesis,[85] primary hippocampal neurons were treated with hNSPC-CM 24 h before application of glutamate (125μM) and CCK8 assay was performed to analyze cell viability (Fig. 10A and B). After exposure to glutamate, an obvious neurotoxicity was observed in primary hippocampal neurons treated with unconditioned culture medium (vehicle vs. glutamate [125μM]; $P < 0.01$; Fig. 10B). The hNSPC-CM protected primary hippocampal neurons against neurotoxicity, but IMR90-CM did not (Fig. 10B), highlighting the potential neuroprotective effect of hNSPC-CM.

Previous studies have shown that neural stem cells constitutively produce and secrete neurotrophic/growth factors with neuroprotective effects against excitotoxic insults.[86-90] We determined the expression patterns of neurotrophic/growth factors secreted by hNSPCs using RT-PCR and Western blot under both proliferation and differentiation conditions (Fig. 10C and D), which revealed that hNSPCs expressed *BDNF*, *NTF3*, *NTF4*, *NGF*, *VEGF*, *FGF2*, and *GDNF* (Fig. 10C). Moreover, BDNF, NTF3, NTF4, NGF, and VEGF protein were detected in hNSPC-CM, but not in IMR90-CM (Fig. 10D), suggesting that these factors could promote neuroprotection observed in hNSPC-grafted epileptic rats.

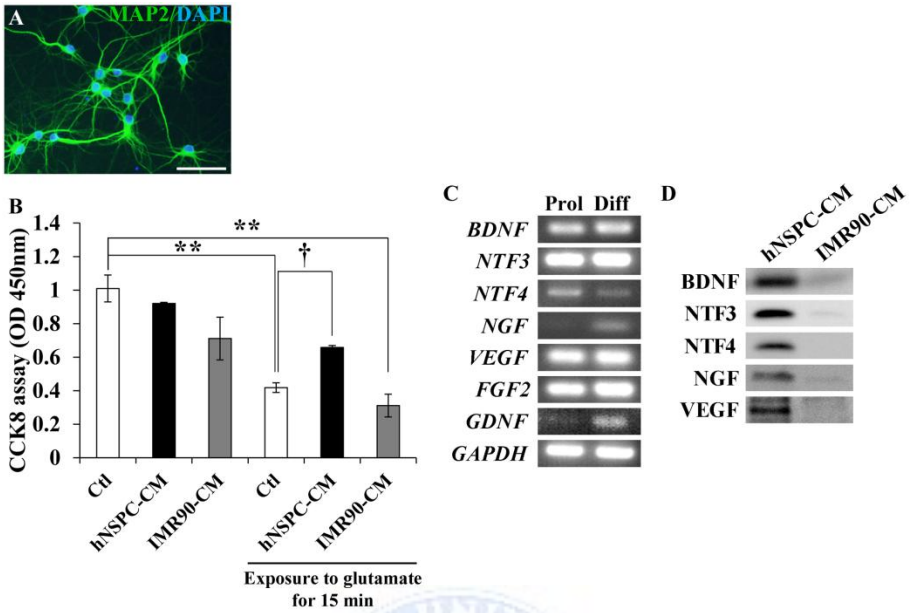

Figure 10. Neuroprotective effect of hNSPCs against glutamate-induced excitotoxicity *in vitro*. (A) Rat primary hippocampal neurons (DIV9) were immunostained with MAP2 antibody. Nuclei were counterstained with DAPI. Scale bar=50 μm. (B) Hippocampal neurons treated with hNSPC-CM, but not IMR90-CM or unconditioned culture medium (control, Ctl), for 24hr were protected against subsequent glutamate excitotoxicity as measured by the CCK8 assay. ** Significantly different from the vehicle-treated Ctl group at $P < 0.01$; † significantly different from glutamate-treated Ctl group at $P < 0.05$; error bars indicate ± SEM. (C) Human NSPCs under proliferation and differentiation conditions *in vitro* expressed neurotrophic/growth factors: BDNF, NTF3, NTF4, NGF, VEGF, FGF2, and GDNF in RT-PCR analysis. (D) BDNF, NTF3, NTF4, NGF, and VEGF proteins were detected in hNSPC-CM, but not in IMR90-CM.

8. Effect of hNSPC grafting on inflammation

Because recent studies have demonstrated that inflammation affects the generation and exacerbation of epilepsy,[91-96] we investigated whether hNSPC grafting could modulate inflammation by controlling its mediators, such as cytokines and chemokines. First, we quantified the expression of hippocampal pro-inflammatory and anti-inflammatory cytokines and chemokines at 21 d after SE, the time of grafting, in lithium-pilocarpine treated and age-matched control rats (Fig. 11A and B). Nine genes encoding cytokines and chemokines were analyzed, and their corresponding protein expression levels (except for IL-1Ra) were determined. Real-time PCR showed the level of *il1b* mRNA was significantly increased, while the levels of *il1rn*, *ifng*, and *ccl5* mRNA were significantly decreased in lithium-pilocarpine treated rats compared to control rats ($P < 0.05$). We observed no significant changes in IL-1β, TNF-α, IL-6, IL-10, IL-4, INF-γ, CXCL8, or CCL5 protein expression levels between lithium-pilocarpine treated and control rats (Fig. 11B).

Next, to elucidate the effects of hNSPC transplantation on inflammation, levels of cytokines and chemokines were measured at 6 and 10 weeks following transplantation in hNSPC- and vehicle-injected rats as described above (Fig. 12). The *il1b* mRNA and protein levels increased at 6 and 10 weeks after injection in the vehicle-injected epileptic group but not in the control (non-epileptic) group (Fig. 12A and D). In contrast, *tnfa* mRNA and protein were expressed similarly in all groups (Fig. 12B and E). Although *il6* mRNA expression was reduced at 6 weeks post-injection in the epileptic group compared to the control group, we did not observe the same difference at 10 weeks after injection (Fig. 12C and F). hNSPC grafting did not affect the expression of pro-inflammatory cytokines, such as IL-1β, TNFα, and IL-6. The level of IL-10 protein in hNSPC-transplanted epileptic rats was significantly increased compared to the vehicle-injected epileptic group and

control group at 6 weeks post-transplants, although *il10* mRNA expression was comparable in all group at both time points (Fig. 12G and J). We noted significantly increased IL-10 protein expression in vehicle- and hNSPC-injected epileptic rats in comparison to control rats at 10 weeks post-transplantation. Levels of *il4* mRNA and protein were higher in both vehicle- and hNSPC-injected epileptic rats than in the control rats at 6 and 10 weeks post-transplants (Fig. 12H and K). Furthermore, *il1rn* mRNA levels were higher at 10 weeks post-transplants in the hNSPC-injected epileptic rats than in the vehicle-injected epileptic rats (Fig. 12I). These results verify hNSPC grafting increased IL-10 protein expression at 6 weeks post-transplants and *il1rn* mRNA expression at 10 weeks post-transplants. Levels of *ifng* mRNA were similar in all groups at 6 weeks post-transplants, and its expression was not detected at 10 weeks following transplantation (Fig. 12L and O). Similarly, its protein expression levels did not significantly differ among the three groups at any time point (Fig. 12O). In contrast, CXCL8 protein expression was markedly increased in epileptic rats at 10 weeks, but not 6 weeks, post-injection compared to control rats (Fig. 12P), while *cxcl8* mRNA levels did not differ among the three groups (Fig. 12M). Compared to the control group, significant increases in *ccl5* mRNA expression were observed in both epileptic groups at 10 weeks, but not 6 weeks, post-transplants (Fig. 12N), although its protein levels significantly increased in both epileptic groups at 6 and 10 weeks post-transplants (Fig. 12Q). These data revealed constant, significant increases of IL-1β, IL-4, and CCL5 levels at 6 and 10 weeks after vehicle and hNSPC injection, and significant increases of IL-10 and CXCL8 levels at 10 weeks after vehicle- and hNSPC-injection in epileptic hippocampus compared to control hippocampus. hNSPC transplantation significantly increased the expression of anti-inflammatory cytokines IL-10 and IL-1Ra at 6 and 10 weeks post-transplants, respectively, in epileptic rats compared to vehicle-injected epileptic rats, however, did not alter the

expression of pro-inflammatory cytokines and chemokines in epileptic hippocampus.

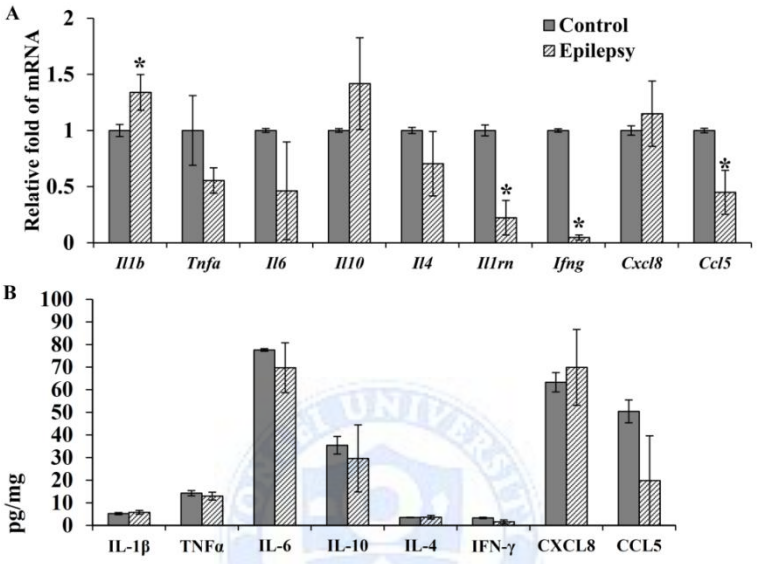

Figure 11. The expression of hippocampal pro-inflammatory and anti-inflammatory cytokines and chemokines (mRNA [A] and protein [B]) at 21 days after SE (the time of vehicle or hNSPC injection) in lithium-pilocarpine-treated epileptic and age-matched control rats. * Significantly different from the control group at $P < 0.05$; error bars indicate ± SEM.

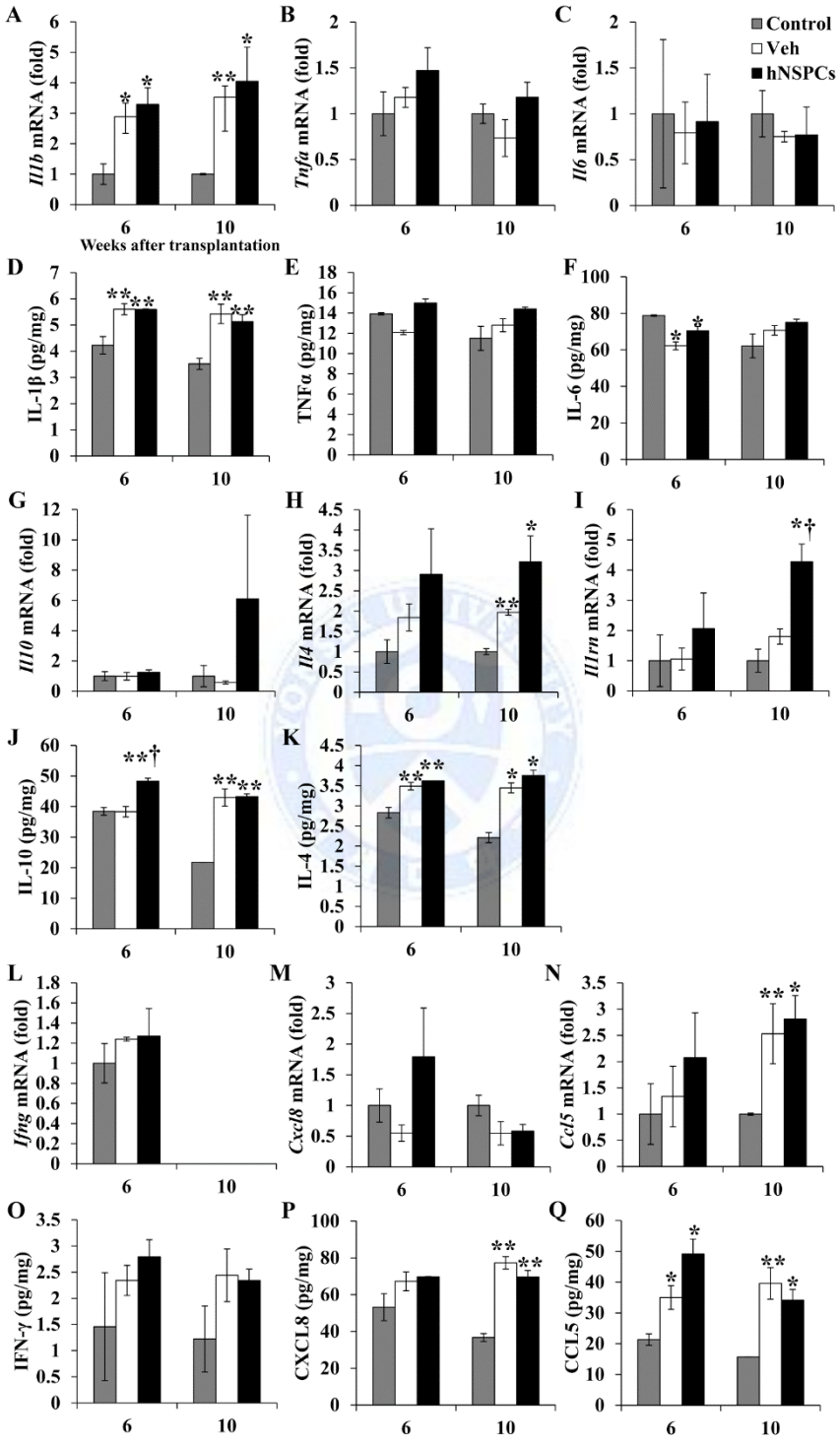
A
Il1b mRNA (fold)
B
Tnfa mRNA (fold)
C
Il6 mRNA (fold)
Control
Veh
hNSPCs
Weeks after transplantation
D
IL-1β (pg/mg)
E
TNFα (pg/mg)
F
IL-6 (pg/mg)
G
Il10 mRNA (fold)
H
Il4 mRNA (fold)
I
Il1rn mRNA (fold)
J
IL-10 (pg/mg)
K
IL-4 (pg/mg)
L
Ifng mRNA (fold)
M
Cxcl8 mRNA (fold)
N
Ccl5 mRNA (fold)
O
IFN-γ (pg/mg)
P
CXCL8 (pg/mg)
Q
CCL5 (pg/mg)

Figure 12. Levels of cytokines and chemokines (mRNA and protein) were measured at 6 and 10 weeks after hNSPC- and vehicle-injection in epileptic rats, and age-matched intact control rats. Note that hNSPC transplantation increased IL-10 protein expression at 6 weeks post-grafting and *il1rn* mRNA expression at 10 weeks following transplantation. * Significantly different from the control group at $P < 0.05$; ** significantly different from the control group at $P < 0.01$; † significantly different from vehicle-injected group at $P < 0.05$; error bars indicate ± SEM.

9. Generation and Characterization of galanin-releasing hNSPCs *in vitro*

GAL-hNSPCs were generated by exposing hNSPCs to Ad-Igκ-GAL-GFP (Fig. 13A). Previous studies have demonstrated that galanin attenuates seizure activity in the hippocampus.[35-38] Thus, we expected that transplantation of GAL-hNSPCs into epileptic hippocampus could exert synergistic effects of hNSPCs and hNSPC-mediated galanin gene therapy on efficiently suppressing seizures in the rat TLE model. We first characterized the GAL-hNSPCs *in vitro* and found that they gave rise to neurospheres (Fig. 13B) and expressed GFP (Fig. 13C). Flow cytometry confirmed that 95% of infected cells expressed GFP. We then analyzed mRNA transcripts expression for human galanin, GALR1, GALR2, and GALR3 in GAL-hNSPCs and GFP-hNSPCs under proliferation and differentiation conditions using RT-PCR (Fig. 13C). Results showed that human galanin mRNA was strongly expressed in only GAL-hNSPCs under both types of conditions. Expression of GALR2 mRNA was observed in GAL-hNSPCs and GFP-hNSPCs, but neither GALR1 nor GALR3 expression was detected. Galanin from the supernatants of GAL-hNSPCs and GFP-hNSPCs was quantified by ELISA (Fig. 13D). The GAL-hNSPCs secreted galanin (4.4 ng/5× 10^5 cells/48 h), whereas no galanin secreted from GFP-hNSPCs was detected.

We determined the effects of galanin secretion on the survival, proliferation, or apoptosis of hNSPCs. The CCK8 assay showed that neither adenoviral infection nor galanin transduction negatively affected hNSPC viability (Fig. 13E). To compare the proliferation rates, we performed EdU labeling experiments on GAL-hNSPCs, GFP-hNSPCs, and non-transfected hNSPCs, which revealed no significant effects of galanin secretion on hNSPC proliferation (Fig. 13F). Further analysis confirmed that galanin transduction did not affect the cell cycle of hNSPCs (Fig. 13G). We also performed TUNEL staining to detect the apoptotic cells and found that very few

TUNEL$^+$ cells (apoptotic cells) were present in GAL-hNSPCs, GFP-hNSPCs, and control cells (Fig. 13H). These data indicate that neither secretion of galanin nor GFP expression alter the viability, proliferation, or apoptosis of hNSPCs.

To examine the differentiation patterns of GAL-hNSPCs *in vitro*, immunocytochemical staining with various cell markers were performed at 7 days after cell plating in the culture dishes under differentiation conditions. The percentage of TUJ1$^+$ neurons (48.0% ± 0.9% vs. 37.8% ± 3.1%; Fig. 14B and E) and OLIG2$^+$ oligodendrocyte progenitors (13.3% ± 1.5% vs. 8.6% ± 0.4%; Fig. 14I and L) significantly increased in GAL-hNSPCs versus GFP-hNSPCs (Fig. 13M). The percentages of GABA$^+$ neurons (13.7% ± 2.5% vs. 10.1% ± 2.5%; Fig. 14C and F), GFAP$^+$ immature cells or astrocytes (60.0% ± 5.1% vs. 60.3% ± 5.1%; Fig. 14G and J), and S100β$^+$ astrocytes (4.2% ± 1.7% vs. 5.3% ± 1.5%; Fig. 14H and K) were similar in GFP-hNSPCs versus GAL-hNSPCs (Fig. 13M). A previous study has reported that galanin promotes neuronal differentiation by increasing in Neurog1 transcript expression.[97] Thus, we evaluated the expression of NEUROG1 mRNA in GAL-hNSPCs under differentiation conditions using real-time PCR. We found that NEUROG1 mRNA levels were significantly elevated in GAL-hNSPCs compared to GFP-hNSPCs, suggesting that galanin could promote neuronal differentiation of hNSPCs through the up-regulation of NEUROG1 transcription (Fig. 13N).

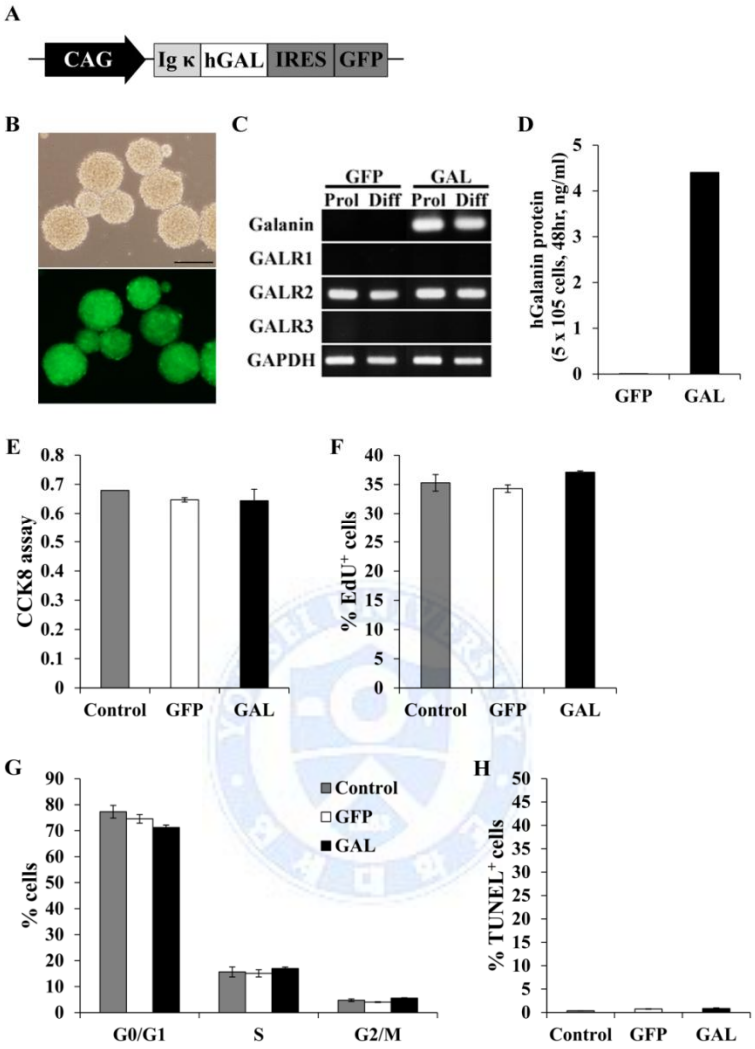

Figure 13. Characterization of galanin-releasing hNSPCs *in vitro*. (A) Structure of adenoviral vector carrying the Igκ leader secretory signal sequence preceding the coding sequence for the active galanin peptide under the control of the CAG promoter and GFP as a reporter, placed under IRES promoter control. (B) Phase and immunofluorescence microscopy of representative neurospheres of GAL-NSPC. Scale bar=100μm. (C) RT-PCR analysis for the expression of human galanin, GALR1, GALR2, and GALR3

in GAL-hNSPCs (GAL) and GFP-hNSPCs (GFP) under proliferation (Prol) and differentiation conditions (Diff). (D) ELISA assay performed using the supernatants of cultured GAL-hNSPCs and GFP-hNSPCs. (E–H) We performed CCK8 assay, EdU labeling experiments, cell cycle analysis, and TUNEL staining with uninfected hNSPCs (control), GFP-hNSPCs and GAL-hNSPCs. Note that neither secretion of galanin nor GFP expression altered the viability, proliferation, or apoptosis of hNSPCs. Error bars indicate ± SEM.

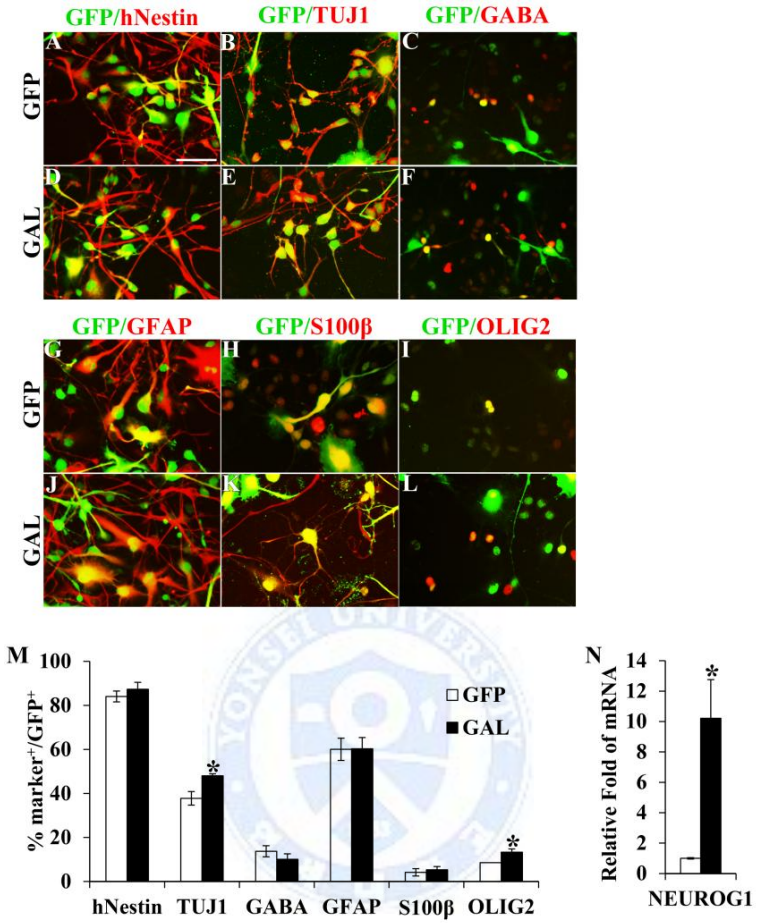

Figure 14. The differentiation patterns of GAL-hNSPCs *in vitro*. (A–M) Percentages of hNestin^{+}-, TUJ1^{+}-, GABA^{+}-, GFAP^{+}-, S100β^{+}-, and OLIG2^{+} cells among total GFP^{+} cells on the immunocytochemical staining with various cell markers were calculated in GFP-hNSPCs (GFP) and GAL-hNSPCs (GAL) under differentiation conditions. (N) Bar graph depicted the relative fold change of mRNA expression for NEUROG1 proneurogenic gene, measured by qRT-PCR analysis under differentiation conditions. * Significantly different from the GFP group at $P < 0.05$; error bars indicate ± SEM.

10. Engraftment and distribution of GAL-hNSPCs following transplantation

Three groups of epileptic rats were injected with vehicle only, GFP-hNSPCs, or GAL-hNSPCs into the CA3 regions of the bilateral hippocampi at 21 days after SE. Immunohistochemical staining with GFP marker revealed that grafted GAL-hNSPCs migrated away from the injection site and dispersed throughout the hippocampus at 3 months post-injection (Fig. 15A). Transplanted GAL-hNSPCs were predominantly located in the radiatum layer of the CA3 region, molecular and granular layers of the DG, and the hilus of the hippocampus (Fig. 15A). To confirm *in vivo* expression of galanin, we performed RT-PCR for Igκ-GAL mRNA in the hippocampus from all groups at 1 month post-injection. As shown in Fig. 15B, hippocampus of epileptic rats with grafted GAL-hNSPCs contained Igκ-GAL mRNA, but those of vehicle-injected or GFP-hNSPC transplanted epileptic rats did not.

11. Differentiation of GAL-hNSPCs in epileptic rats following transplantation

We examined the differentiation patterns of GAL-hNSPCs following transplantation into the hippocampus in epileptic rats. In whole hippocampal areas of epileptic rats that received GAL-hNSPCs, GFP^+ grafted cells expressed nestin (66.4% ± 13.9%; Fig. 16A–D), TUJ1 (27.4% ± 4.7%; Fig. 16E–H), GFAP (60.9% ± 9.8%; Fig. 16 I–L), OLIG2 (9.3% ± 3.2%; Fig. 16 M–P), and GABA (22.0 ± 2.7%; Fig.16 Q–T) in the hippocampus. Compared to the GFP-hNSPC-transplanted epileptic rats, significantly higher number of grafted cells differentiated into $TUJ1^+$ neurons and $OLIG2^+$ oligodendrocyte progenitors by 15.7% and 8.4%, respectively, and lower number of grafted cells expressed nestin by 18.6% in the GAL-hNSPCs-transplanted group (Fig. 16U). In both groups, few GFP^+ cells (about 1%) expressed astrocyte marker S100β.

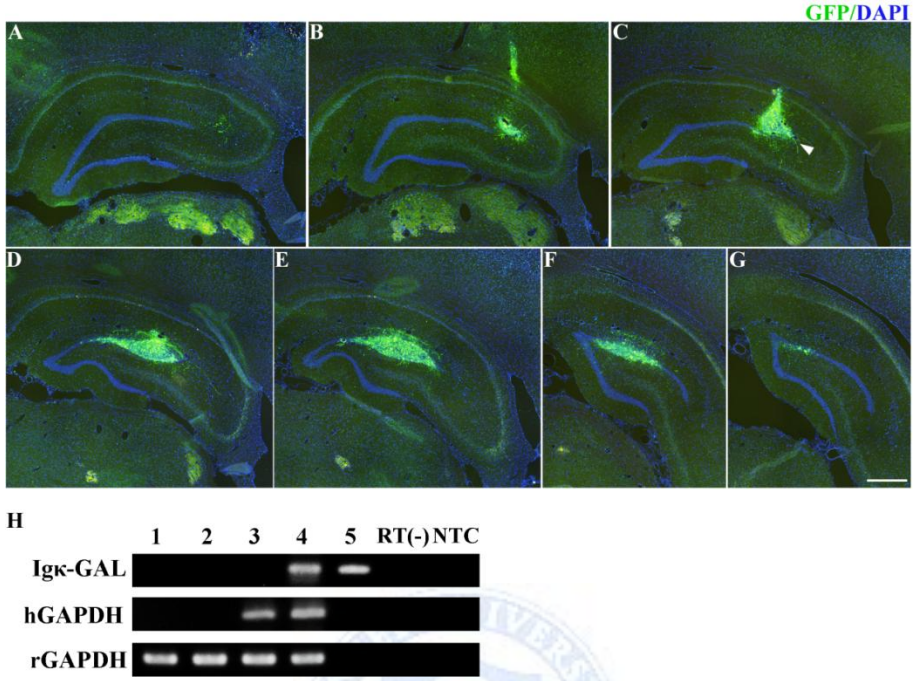

Figure 15. Engraftment and distribution of GAL-hNSPCs after transplantation into the epileptic hippocampus, and *in vivo* expression of Igκ-GAL mRNA. (A–G) Serial sections (320μm) through the hippocampus showed the location of GFP^+ grafted cells at 3 months post-transplants. Nuclei were counterstained with DAPI. The arrowhead indicates the injection site. Scale bar=500μm. (H) The *in vivo* presence of Igκ-GAL mRNA at 1 month post-transplants into the hippocampus in RT-PCR. Igκ-GAL mRNA expression was detected in GAL-hNSPC-grafted hippocampus (lane 4), but not age-matched intact control (lane 1), vehicle- (lane 2) and GFP-hNSPC- (lane 3) injected hippocampus. Plasmid DNA containing the Igκ-GAL sequence was used as positive control for Igκ-GAL-specific RT-PCR (lane 5). Omission of the RT step (RT(-)) indicated the absence of contaminating viral DNA. No template control (NTC) was used as negative control.

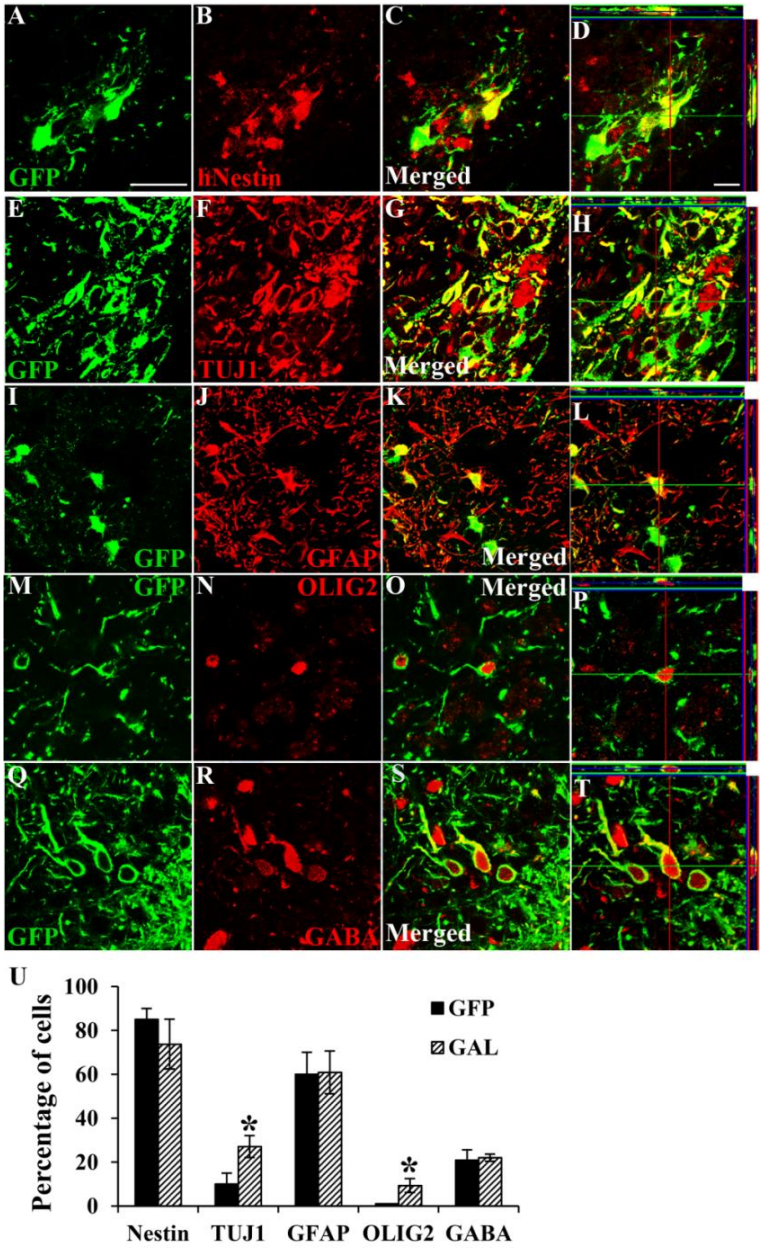

Figure 16. Differentiation of GAL-hNSPCs in epileptic rats following transplantation. (A–T) GFP^+ cells (green) co-expressed hNestin, TUJ1, GFAP, OLIG2, and GABA (all in red). Orthogonal view from confocal *z*-series

showed that GFP and cell type-specific markers were expressed in the same cell. Scale bar=50 μm (A), 20 μm (D). (U) Comparison of differentiation patterns between GAL-hNSPC (GAL) and GFP-hNSPC (GFP) transplantation groups. * Significantly different from the GFP-hNSPC transplantation group at $P < 0.05$; error bars indicate ± SEM.

12. Effect of GAL-hNSPC transplantation on SRMS and behavioral abnormalities

We conducted video monitoring to document the frequency and duration of SRMS in the epileptic rats for 3 months following transplantation. In vehicle-injected rats (n = 30), mean SRMS frequencies evaluated at 1, 2, and 3 months after injection were 0.90 ± 0.30, 0.92 ± 0.30, and 1.12 ± 0.35 seizures per day, respectively (Fig. 17A). In GAL-hNSPC- and GFP-hNSPC-injected rats (n = 12 and 17, respectively), mean SRMS frequencies evaluated at 1, 2, and 3 months after injection were 0.08 ± 0.04 and 0.42 ± 0.13, 0.03 ± 0.01 and 0.31 ± 0.07, and 0.15 ± 0.08 and 0.21 ± 0.09 seizures per day, respectively (Fig. 17A). Thus, the epileptic rats that received GAL-hNSPC grafting exhibited remarkable reductions in SRMS frequency in comparison to epileptic rats that received vehicle or GFP-NSPC injection at 1 and 2 months following transplantation ($P < 0.05$). These observations indicated a significant attenuation of SRMS frequency via galanin-secreting hNSPC transplantation. Additionally, mean SRMS frequencies in both GAL-hNSPC and GFP-hNSPC transplantation groups were significantly lower compared to those of vehicle-injected group at 3 months post-transplants ($P < 0.05$). However, the mean SRMS frequencies at this time point were not significantly different between GAL-hNSPC and GFP-hNSPC transplantation groups. We observed similar results with respect to total time spent in SRMS (Fig. 17B). Seizure severity was usually stage 4 or 5 in all three groups which consequently showed no significant difference among three groups (Fig. 17C).

We also investigated whether GAL-NSPC transplantation affected the rats' performance in a Morris water maze test, which assesses hippocampal-dependent learning and memory function, at 3 months following transplantation (Fig. 17D–H). As discussed above, vehicle-injected epileptic rats exhibited significantly impaired learning ability in the hidden platform

test (Fig. 17D), and epileptic rats that received GAL-hNSPC or GFP-hNSPC grafting did not show improvement in the learning deficits. This learning impairment was confirmed in the probe test (Fig. 17E–H), in which the vehicle-injected epileptic rats spent less time in the target quadrant and platform area (Fig. 17E and F), took longer to reach the platform area (Fig. 17G), and crossed the platform area in less time (Fig. 17H) when the platform was removed. Epileptic rats in the GAL-NSPC and GFP-NSPC transplantation groups also showed significantly poor performance in the probe test. Thus, GAL-NSPC or GFP-NSPC grafting did not ameliorate learning and memory impairment as observed in the vehicle-injected epileptic rats.

Additionally, we performed the elevated plus maze test to evaluate anxiety related-behavior in epileptic rats at 3 months following transplantation. A vehicle-injected rat and two GFP-hNSPC-injected rats were excluded from the analysis because they jumped off the maze. Vehicle-injected rats spent more time in the open arms (Fig. 17I), indicating reduced anxiety level. Consistent with our data, previous studies reported that pilocarpine-induced epileptic rats exhibited the lower level of anxiety in the elevated plus maze compared to non-epileptic control rats.[5,33,98] Time spent in the open arms was not significantly different between GFP-hNSPC- and vehicle-injected epileptic rats. In contrast, the time spent in the open arms was significantly lower in GAL-hNSPC-injected epileptic group compared to vehicle- and GFP-hNSPC-injected epileptic groups ($P < 0.05$). Thus, GAL-NSPC transplantation reversed the decreased anxiety levels of the epileptic rats.

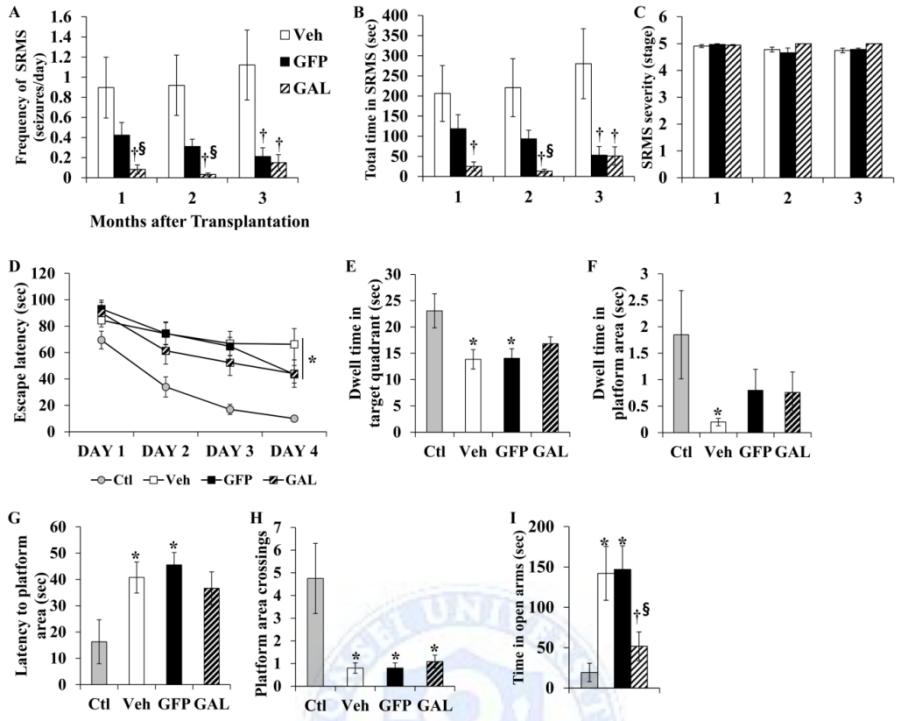

Figure 17. Effects of GAL-hNSPC transplantation into the hippocampus on SRMS, anxiety-like behavior, spatial learning and memory function in the epileptic rats. (A–C) The mean seizure frequencies (A), total time spent in seizures (B) and seizure stages (C) were calculated during 1, 2, and 3 months following injection in vehicle (Veh)-, GFP-hNSPC (GFP)-, and GAL-hNSPC (GAL)-injected epileptic rats. (D) In a Morris water maze test, hidden platform test showed significantly impaired learning ability in vehicle-, GFP-hNSPC, and GAL-hNSPC-injected epileptic rats compared to non-epileptic controls (Ctl). (E–H) During probe testing on day 5, dwell time in the target quadrant (E) and platform area (F), latency to the platform (G), and platform area crossings (H) were measured in the four groups. All three epileptic groups (Veh, GFP and GAL) exhibited significant deficits in memory retention. (I) In the elevated plus maze test, vehicle-injected epileptic rats exhibited a lower level of anxiety compared to non-epileptic control rats. This

was reversed by GAL-hNSPC transplantation, but not by GFP-hNSPC transplantation. * Significantly different from Ctl at $P < 0.05$; † significantly different from Veh at $P < 0.05$; § significantly different from GFP at $P < 0.05$; error bars indicate ± SEM.

13. Effect of GAL-hNSPC transplantation on histopathological changes in the hippocampus

To determine whether GFP-hNSPC or GAL-hNSPC transplantation influences neuropathological alterations, we analyzed the neuronal damage, MFS, and neurogenesis in the hippocampus of the epileptic rats in the vehicle- (n = 8), GFP-hNSPC- (n = 10), and GAL-hNSPC- (n = 8) injected groups at 3 months following injection. Immunohistochemical staining with anti-NeuN antibody and quantitative analysis revealed significantly reduced neuronal density in the pyramidal cell layer of CA3c, CA3ab, and CA1 regions, and in the hilus of the DG in vehicle-injected epileptic rats compared to age-matched intact control rats (n = 4; Fig. 18A, B, E, F and I). In the GFP-hNSPC-injected group, neuronal loss in CA3c region was significantly decreased compared to the vehicle-injected group ($P < 0.05$; Fig. 18C and G), however, GAL-hNSPC transplantation significantly decreased neuronal loss in both CA3c and CA3ab regions of the hippocampus compared to the vehicle-injected group ($P < 0.05$; Fig. 18D and H), leading to a more pronounced neuroprotective effect of GAL-hNSPC-injected group than GFP-hNSPC-injected group. Additionally histological quantification revealed that the number of PV^+ neurons in the hilus, CA3, and CA1 regions of the hippocampus was not significantly different among all three epileptic groups, however, all three epileptic groups showed fewer PV^+ neurons in the subfields of the hippocampus than those in the intact control group (data not shown; $P < 0.05$).

Immunohistochemical staining with ZnT3 showed that robust MFS was present in the IML of the DG in all epileptic rats, however, not in non-epileptic control rats (Fig. 19A–H). The quantification of the data showed that the degree of MFS was significantly lower in the GFP-hNSPC- and GAL-hNSPC-grafted groups than the vehicle-injected group ($P < 0.05$ and $P < 0.01$, respectively; Fig. 19I). However, no significant difference was found in the

degree of the MFS between GFP-hNSPC- and GAL-hNSPC-grafted rats. Collectively, these results show that transplantation of hNSPCs into the epileptic hippocampus can suppress the degree of the aberrant MFS.

14. Effect of GAL-hNSPC transplantation on neurogenesis in the hippocampus

A previous study demonstrated that galanin enhanced neurogenesis in cultured hippocampal NSPCs,[99] thus we then tested whether GAL-hNSPC transplantation into the hippocampus affects hippocampal neurogenesis at 3 months following transplantation. Immunohistochemical staining with anti-DCX antibody identifies the newly born neurons, and DCX^+GFP^- newly born host cells were distinguished from grafted hNSPC-derived DCX^+ cells. Histological quantification showed that the number of DCX^+ neurons in the SGZ-GCL of the DG significantly declined by 62% in vehicle-injected (n = 8, $P < 0.001$; Fig. 20B), by 66% in GFP-hNSPC-injected (n = 10, $P < 0.001$; Fig. 20C), and by 33% in GAL-hNSPC-injected rats (n = 8, $P < 0.05$; Fig. 20D) when compared with non-epileptic control rats (Fig. 20A). We observed no significant difference in DCX^+GFP^- newly born neurons in the SGZ-GCL of the DG between vehicle- and GFP-hNSPC-injected groups (Fig. 20I). In contrast, the GAL-hNSPC-injected group had approximately twice as many DCX^+GFP^- neurons compared to vehicle and GFP-hNSPC-injected groups ($P < 0.001$ and $P < 0.05$, respectively; Fig. 20E), suggesting that GAL-hNSPC transplantation can partially reverse impaired neurogenesis levels in the DG of chronic epileptic hippocampus.

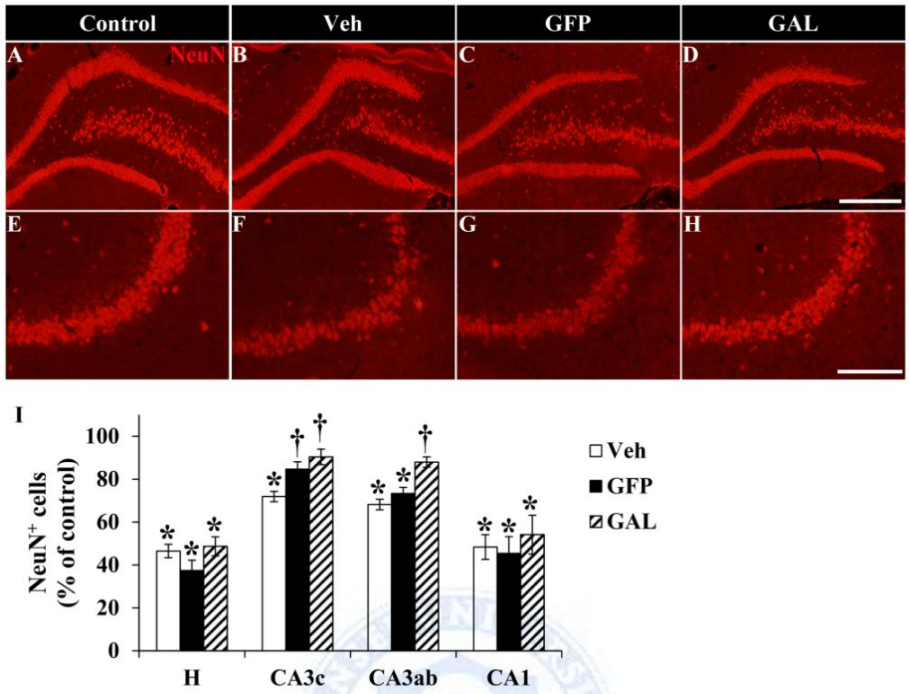

Figure 18. Effect of GAL-hNSPC transplantation on neuronal damage in the hippocampus of the epileptic rats. (A–H) Representative sections of NeuN immunostaining in the CA3c and CA3ab regions of the intact control (A and E, respectively), vehicle-injected epileptic (B and F, respectively), GFP-hNSPC-injected epileptic (C and G, respectively), and GAL-hNSPC-injected epileptic rats (D and H, respectively). (A–D and I) GFP-hNSPC (GFP) and GAL-hNSPC (GAL) transplantation significantly relieved $NeuN^+$ neuronal loss in the pyramidal cell layer of CA3c region compared to vehicle-injected group (Veh). (E–H and I) GAL-hNSPC transplantation significantly relieved NeuN+ neuronal loss in the pyramidal cell layer of CA3ab region compared to vehicle-injected group. * Significantly different from control at $P < 0.05$; † significantly different from vehicle-injected group at $P < 0.05$; error bars indicate ± SEM. Scale bar=200 μm (D), 100 μm (H).

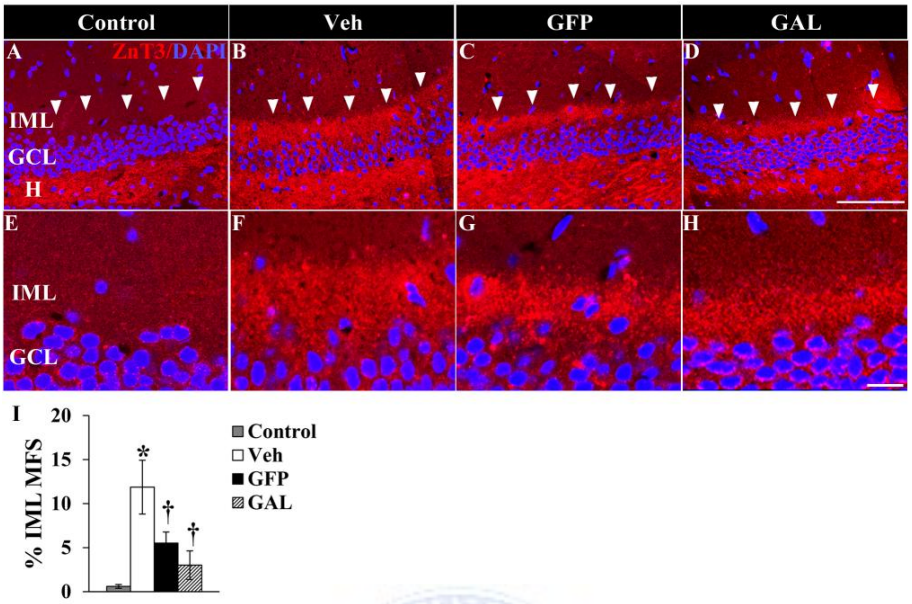

Figure 19. Effect of GAL-hNSPC and GFP-hNSPC transplantation on MFS in the epileptic hippocampus. (A–H) Representative sections of ZnT3 immunostaining in the IML of the DG in intact control (A and E), vehicle-injected epileptic (B and F), GFP-hNSPC-injected epileptic (C and G), and GAL-hNSPC-injected epileptic rats (D and H). (I) Bar graphs illustrate the quantification of MFS in the IML of the DG in the control and experimental groups. The degree of MFS was significantly lower in the GFP-hNSPC (GFP) and GAL-hNSPC (GAL) transplantation groups than the vehicle-injected group (Veh). No robust MFS was present in the IML of the DG in control rats (Control). * Significantly different from control at $P < 0.05$; † significantly different from vehicle-injected group at $P < 0.05$; error bars indicate ± SEM. Abbreviations: IML, inner molecular layer; GCL, granular cell layer; H, hilus. Scale bar=100 μm (D), 20 μm (H).

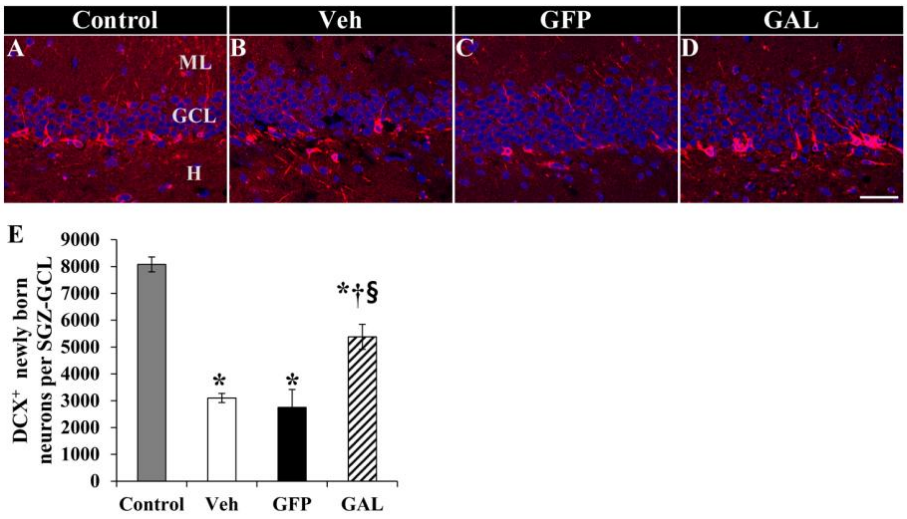

Figure 20. Effect of GAL-hNSPC transplantation on neurogenesis in the epileptic hippocampus. The number of DCX^+ newly neurons in the SGZ-GCL of the DG significantly declined in vehicle- (B), GFP-hNSPC- (C), and GAL-hNSPC- (D) injected epileptic rats compared to non-epileptic control rats (A). (E) Bar graphs illustrate the quantification of DCX^+ newly neurons in the SGZ-GCL of the DG in the control and experimental groups. * Significantly different from control at $P < 0.05$; † significantly different from vehicle-injected group at $P < 0.05$; § significantly different from GFP-hNSPC-injected group at $P < 0.05$; error bars indicate ± SEM. Abbreviations: ML, molecular layer; GCL, granular cell layer; H, hilus. Scale bar=20 μm.

15. Effect of GAL-hNSPC transplantation on the expression of GDNF in host hippocampal astrocytes

As described above, transplantation of hNSPCs into LV restored GDNF expression in the majority of hippocampal astrocytes in the epileptic rats. Thus, we also examined whether transplantation of GFP-hNSPCs or GAL-hNSPCs into the hippocampus would induce GDNF expression in host hippocampal astrocytes. Immunohistochemical staining with anti-S100β and anti-GDNF antibodies was performed at 3 months following transplantation. Histological quantification revealed that the number of $GDNF^{+}S100\beta^{+}$ astrocytes among total $S100\beta^{+}$ astrocytes significantly decreased in vehicle-injected rats (n = 8; Fig. 21E-H) compared to non-epileptic control rats (n = 6; Fig. 21A-D) in the DG (48% vs. 75%, $P < 0.05$), CA3 (44% vs. 72%, $P < 0.05$), and CA1 (65% vs. 79%, $P < 0.05$) regions of the hippocampus (Fig. 21Q). When compared to the vehicle-injected group, percentages of $GDNF^{+}S100\beta^{+}$ astrocytes were significantly higher in the DG (71%) and CA3 (76%) regions of the GFP-hNSPC-injected group (n = 8, $P < 0.05$; Fig. 21I–L), as well as in the CA1 (83%) region of GAL-hNSPC-injected rats (n = 6, $P < 0.05$; Fig. 21M–P). These results showed that transplantation of GFP-hNSPCs or GAL-hNSPCs into the CA3 region of the hippocampus can restore GDNF expression in host hippocampal astrocyte which may be contributed to suppress seizures.

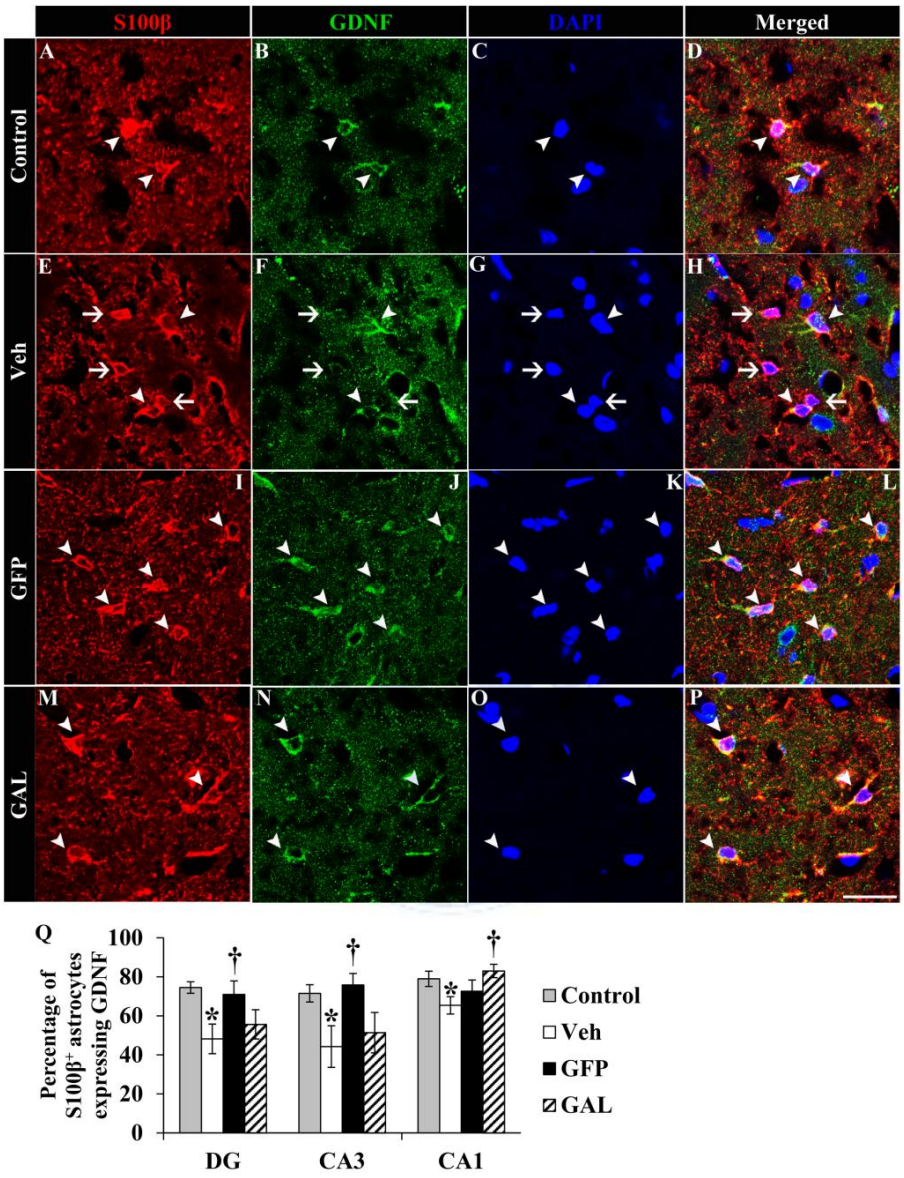

Figure 21. Effect of GFP-hNSPC and GAL-hNSPC transplantation into the epileptic hippocampus on the expression of GDNF in host hippocampal astrocytes. GDNF expression in S100β^{+} hippocampal astrocytes was observed in age-matched intact control (A–D), vehicle- (E–H), GFP-hNSPC- (I–L), and GAL-hNSPC- (M–P) injected-epileptic rats. Nuclei were counterstained with

DAPI (C, G, K and O). Arrowheads in A-L indicated S100β/GDNF double-labeled cells. Arrows in E, G and H denoted $S100\beta^+$ host hippocampal astrocytes that were devoid of GDNF immunoreactivity in vehicle-injected rats. Scale bar=50 μm. (Q) The bar chart represents percentages of $S100\beta^+$ astrocytes expressing GDNF in the hippocampal subfields in the three experimental groups. * Significantly different from the age-matched intact control group at $P < 0.05$; † significantly different from vehicle-injected group at $P < 0.05$; error bars indicate ± SEM.

IV. DISCUSSION

hNSPCs grafted into the LV of epileptic brains exerted a therapeutic effect by suppressing SRMS in the rat lithium-pilocarpine model of TLE. This effect might be related to substantial preservation of the pyramidal neurons and PV^+ interneurons, restoration of GDNF expression in hippocampal astrocytes, and up-regulation of anti-inflammatory cytokines, such as IL-10 and IL-1Ra. We also observed that intrahippocampal injection of either GFP-hNSPCs or GAL-hNSPCs reduced the frequency and duration of SRMS with an addition of GABA-expressing cells into the hippocampus, a considerable preservation of the pyramidal neurons, and a significant reduction of MFS, which highlights the beneficial effects of these cells in this model. We also found that galanin secreted by hNSPCs enhanced their therapeutic effectiveness, as the GAL-hNSPC-injected group experienced more prompt seizure control, extensive neuroprotection, recovery of emotional deficit, and reversal of decreased neurogenesis that were not observed in GFP-hNSPC-injected group.

Several studies demonstrated that loss of inhibitory interneurons is seen commonly in the hippocampus of TLE animal models and patients with epilepsy.[80,100-102] PV^+ cells, a subset of GABAergic interneurons, are lost during chronic epilepsy[103] that directly correlates to the severity of seizures.[7] In our study, vehicle-injected epileptic rats experienced severe loss of PV^+ cells in the hilus, CA3, and CA1 regions of the hippocampus compared to control rats while no loss of PV^+ cells was observed in the CA3 and CA1 regions in hNSPC-injected epileptic rats. Thus, substantial preservation of PV^+ cells in the hippocampus mediated by hNSPC grafting could play a role in the seizure-restraining effects in this group.

A prior study reported that rat fetal MGE-derived NSCs grafting into rats with chronic epilepsy restrained SRS by suppling new donor-derived $GDNF^+$ cells with recovery of GDNF expression in host hippocampal astrocytes.[10] We

observed a few hNSPC-derived cells differentiated into GDNF^{+} astrocytes when hNSPCs were injected into the LV. However, hNSPC transplantation induced GDNF expression in the hilus, CA3, and CA1 regions of the host hippocampus in epileptic rats. hNSPCs express FGF-2 at a high level, which induces GDNF expression in astrocytes.[104,105] Increased GDNF levels in the hippocampal astrocytes restrain seizures,[83,84] which indicates that induced GDNF expression in host hippocampal astrocytes by hNSPC grafting may be involved in seizure suppression.

Because other studies have shown that inflammation plays a role in generation and exacerbation of epilepsy,[91-96] we tested whether hNSPC grafting modulates the inflammation by controlling inflammatory mediators, such as cytokines and chemokines. At the time of grafting (21 days post-SE) the level of *il1b* mRNA, but not protein, was significantly increased in the epileptic rats. This discrepancy between the mRNA and protein expression levels could be attributed to post-translational regulatory mechanisms involved in the release of IL-1β.[106] Before hNSPC transplantation, there were no significant changes in protein levels of IL-1β, TNF-α, IL-6, IL-10, IL-4, INF-γ, CXCL8, or CCL5 between epileptic and control rats. In contrast, at 6 and 10 weeks after injection, we observed significantly increased mRNA and protein levels of IL-1β, but not other pro-inflammatory cytokines, TNF-α and IL-6, in vehicle-injected epileptic rats as reported in a previous study.[91] Expression of pro-inflammatory chemokines CXCL8 and CCL5 were also up-regulated in vehicle-injected epileptic rats. hNSPC grafting significantly increased expression of the anti-inflammatory cytokines IL-10 and IL-1Ra at 6 and 10 weeks post-transplantation, respectively. Previous studies reported that intracerebral injections of IL-1Ra or transgenic overexpression of astrocytic IL-1Ra exerts anticonvulsant effects.[91,107] Thus, up-regulation of IL-1Ra in the hippocampus of hNSPC-grafted epileptic rats may be related to the seizure suppression effect we observed in this study.

When transplanted into the LV, hNSPC-derived cells robustly integrated into the epileptic brain, and distributed in the SVZ, the corpus callosum, fimbria of the hippocampus, the neocortex, and the external capsule. The majority of hNSPCs remained undifferentiated, although subsets of the donor-derived cells expressed neuronal and glial lineage markers. Thus, we hypothesized that the therapeutic effects of hNSPC transplantation are most likely due to paracrine mechanisms, rather than cell replacement. Several studies have demonstrated that neurotrophic growth factors secreted by neural stem/progenitor cells can protect against neuronal cell death and promote functional recovery in animal models of neurodegenerative disorders.[108-111] In this study, we found that hNSPCs expressed neurotrophic/growth factor such as BDNF, NTF3, NTF4, NGF, VEGF, FGF2, and GDNF, suggesting that paracrine factors secreted by hNSPCs might preserve pyramidal neurons and PV^+ interneurons, and in part, aid in the maintenance of a functional neural network. The proposed paracrine mechanism in hNSPC-transplanted rats is supported by the observed neuroprotective effect of hNSPC-CM against excitotoxic insult *in vitro*. In addition, FGF2 released from hNSPCs could indirectly suppress seizures by inducing GDNF expression in hippocampal astrocytes in epileptic rats. Furthermore, neural stem/progenitor cells produce endogenous cannabinoids (CBs),[112,113] which provide neuroprotection against excitotoxicity by inducing IL-1Ra release from neurons or glial cells.[114] These studies suggest that the up-regulation of IL-1Ra in epileptic hippocampus of hNSPC-grafted epileptic rats could be related to secretion of CBs by hNSPCs.

Galanin, a neuropeptide that acts as an inhibitory neuromodulator, attenuates seizure activity in the hippocampus.[35-38] Moreover, GALR1 and GALR2 are expressed in the hippocampus and contribute to inhibit epileptic activity.[40] AAV–mediated gene therapy utilizing galanin has been used to treat animal models with TLE and acute seizures.[35,44,45] For example, an AAV vector carrying the fibronectin secretory signal sequence (FIB) preceding the

coding sequence for the active galanin peptide (AAV-FIB-GAL) significantly reduced *in vivo* focal seizure sensitivity and prevented KA-induced hilar cell death.[35] Recently, a report demonstrated that developing encapsulated galanin-producing cells was advantageous because of no direct genetic modification of the host cells by viral vector-based delivery and no need for immunosuppressant drugs.[36] In contrast to encapsulated cell grafts, which provide a moderate anti-convulsant effect exclusively by paracrine action, neural stem cell grafts may survive long term, migrate, and integrate into the hippocampus and directly influence seizure activity. Therefore, to combine hNSPC and galanin-mediated gene therapy, we developed GAL-hNSPCs using adenoviral vector. GAL-hNSPCs retained the characteristics of hNSPC, exhibiting self-renewal and multipotency. Under differentiation conditions *in vitro*, GAL-hNSPCs experienced galanin-enhanced neuronal and oligodendroglial differentiation compared to GFP-hNSPCs, consistent with a previous study showing that galanin promoted neuronal differentiation of SVZ neural stem cells.

To avoid systemic side effects and optimize anticonvulsant effects, focal administration of GAL-hNSPCs into the hippocampus was needed. Thus, we transplanted GAL-hNSPCs and GFP-hNSPCs into the CA3 region of the bilateral hippocampus. Labeling with GFP revealed that grafted GAL-hNSPCs migrated away from the injection site and dispersed throughout the hippocampus at 3 months post-injection. *In vivo* expression of Igκ-GAL mRNA was confirmed in hippocampal tissue by RT-PCR because *in vivo* expression and secretion of galanin did not prove amenable to immunohistochemical localization detection.[35,44] The hippocampus of epileptic rats that received GAL-hNSPCs contained Igκ-GAL mRNA, but those of vehicle-injected or GFP-hNSPC transplanted epileptic rats did not. Either GFP-hNSPCs or GAL-hNSPCs differentiated into $TUJ1^+$, $GFAP^+$, $OLIG2^+$, and $GABA^+$ cells. Interestingly, among the donor-derived cells, the

fraction of TUJ1^{+} or OLIG2^{+} cells were increased in GAL-hNSPC transplanted group compared to GFP-hNSPC transplanted group. It might be associated with up-regulation of NEUROG1 in GAL-hNSPCs. Importantly, GFP-hNSPCs and GAL-hNSPCs expressed GABA (20.8% and 22.0%, respectively). This is substantial because GABAergic function decreases in TLE,[115-117] and grafted cells that release GABA could facilitate anti-seizure effects.

GFP-hNSPC transplantation attenuated the frequency and duration of SRMS from 1 month post-transplant and showed significance at 3 months, while GAL-hNSPC transplantation significantly reduced SRMS through all the time period. Moreover, GAL-NPSC transplantation reversed the decreased anxiety level in epileptic rats. These results suggest that GAL-hNSPCs are an improved hNSPC and gene therapy strategy for TLE.

Histopathological analysis revealed that more extensive neuroprotection in CA3 occurred in GAL-hNSPC rats than GFP-hNSPC rats, indicating that galanin enhances neuroprotection *in vivo*. This finding is consistent with a previous study describing the neuroprotective activity of galanin in the hippocampus.[118] MFS, which is linked to increased seizure susceptibility during TLE,[119] was suppressed by both GFP-hNSPC and GAL-hNSPC grafting. In the pilocarpine model, MFS began to appear early after SE and reached a plateau by 100 days.[8] Previous studies demonstrated that fetal hippocampal cells grafted into the hippocampus resulted in neuronal differentiation in CA3 and partial reversal of aberrant MFS, possibly by providing an appropriate target.[120,121] We observed that transplanted GFP-hNSPCs and GAL-hNSPCs differentiated into TUJ1^{+} neurons in the CA3 region, which may linked to suppress MFS seen in the GFP-hNSPC and GAL-hNSPC group. Chronic TLE is associated with dramatically decreased neurogenesis in the DG of the hippocampus, which might contribute to the increased seizure susceptibility of the DG and hippocampal-dependent

learning and memory deficits.[9,10] Our study also supports these findings as the number of newly generated neurons significantly declined in vehicle-injected epileptic rats compared to control rats, indicating decreased neurogenesis due to epilepsy. The GAL-hNSPC group experienced a partial reversal of decreased neurogenesis, but the GFP-hNSPC group did not, suggesting that galanin induces hippocampal neurogenesis. This result is corroborated by a previous study describing galanin-enhanced neurogenesis in cultured hippocampal NSPCs.[99] In contrast, Morris water maze testing revealed that learning and memory impairment was present in all epileptic rats, although GAL-hNSPC rats showed slightly shorter escape latencies than the vehicle group in the hidden platform test. Learning and memory deficits were not significantly improved in these rats compared to non-epileptic controls. This lack of improvement may be attributed to the partial, but not complete, restoration of decreased neurogenesis.

Grafting of hNSPCs into the LV restored GDNF expression in a substantial majority of hippocampal astrocytes in the hilus, CA3, and CA1 regions of the epileptic hippocampus. In contrast, the fraction of GDNF-expressing $S100\beta^{+}$ astrocytes were significantly increased in the hilus and CA3 regions of the GFP-hNSPC rats, and in CA1 region of the GAL-hNSPC rats, indicating that restoration of GDNF expression was less apparent in intrahippocampal grafting of GFP-hNSPCs or GAL-hNSPCs than in intracerebroventricular transplantation of hNSPCs. Down-regulation of FGF-2, a factor that may induce GDNF expression, in genetically modified hNSPCs could be responsible for this difference and will be investigated in future studies.

Grafting of GAL-hNSPC or hNSPC grafting could not restore spatial learning and memory function in rats with TLE. Other studies reported a marked reduction in seizures and some reversal of behavioral deficits, including spatial learning and memory function, when transplanted mouse

fetal MGE precursor cells differentiated into mature inhibitory interneurons and integrated functionally into the existing hippocampal neuronal network.[23] Thus, new strategies of hNSPC grafting should be developed to provide graft-derived mature GABAergic interneurons, which functionally integrate into epileptic hippocampal circuitry, to induce not only seizure suppression but also relieve cognitive deficiencies in epileptic models.

In summary (Table 3), our results provide evidence that hNSPC transplantation into the LV has potential therapeutic effects for managing TLE, with regard to seizure suppression. These benefits may result from neuroprotection, restoration of astrocytic GDNF expression, and anti-inflammatory action in the epileptic hippocampus mediated by hNSPCs, although the majority of the donor-derived cells remained undifferentiated. Furthermore, this study provides the first evidence that galanin-secreting hNSPC transplantation into adult epileptic rat brain exerts therapeutic effects against SRMS and emotional deficit and for increasing neurogenesis and neuroprotection in the hippocampus of the lithium-pilocarpine induced TLE model, representing a novel combined stem cell and gene therapy in severely epileptic rats.

Table 3. Results of grafting of hNSPCs or GAL-hNSPCs in epileptic rats

Approach	Result	Presumed mechanism
hNSPCs into LV	1 mo: no effect on sz 2 mo: 86% sz ↓ 3 mo: 75% sz ↓	New GABA-expressing cells; Preservation of $NeuN^+$ neurons in CA3c and of PV^+ interneurons in CA1; Restoration of astrocytic GDNF expression; Up-regulation of IL-10 and IL-1Ra
hNSPCs into HI	1 mo: 53% sz ↓ 2 mo: 66% sz ↓ 3 mo: 81% sz ↓	New GABA-expressing cells; Preservation of $NeuN^+$ neurons in CA3c; Restoration of astrocytic GDNF expression; Suppression of MFS
GAL-hNSPCs into HI	1 mo: 91% sz ↓ 2 mo: 96% sz ↓ 3 mo: 87% sz ↓; Recovery of emotional deficit; Enhanced neurogenesis	Increase of local galanin levels; New GABA-expressing cells; Preservation of $NeuN^+$ neurons in both of CA3ab and CA3c; Restoration of astrocytic GDNF expression; Suppression of MFS

Abbreviations: LV, lateral ventricle; HI, hippocampus; sz, seizure; PV, parvalbumin; IL-1Ra, IL-1 receptor antagonist; GDNF, glial cell derived neurotrophic factor; MFS, mossy fiber sprouting.

V. CONCLUSION

NSPC-based therapy in animal models of epilepsy shows anticonvulsant and antiepileptogenic effects, replacing degenerated neurons, repairing damaged neural circuitry, and modulating neurotrophic expression. However, prior to the clinical application of NSPCs for epilepsy treatment, it is essential to study hNSPCs derived from various cell sources for their abilities in terms of engraftment, migration, differentiation into specific neuronal or glial cells, seizure control, and cognitive or neurobehavioral recovery following transplantation into the brains of TLE models.

In the present study, we first transplanted hNSPCs into the LV of the rat lithium-pilocarpine model of TLE after SRMS emerged. Grafted cells were found in the SVZ, fimbria of the hippocampus, the corpus callosum, the neocortex, and the external capsule at 3 months post-transplants, indicating robust engraftment, long-term survival, and extensive migration of grafted cells. In terms of differentiation, the majority of hNSPCs remained undifferentiated, although subsets of grafted cells not only expressed neuronal or glial lineage markers, but also differentiated into GABA-expressing cells. hNSPCs transplantation into the LV of epileptic brains significantly reduced the frequency and duration of SRMS. hNSPC-transplanted epileptic rats showed substantial preservation of $NeuN^+$ neurons and PV^+ interneurons, restoration of GDNF expression in astrocytes, and up-regulation of anti-inflammatory cytokines in the hippocampus. In addition, the hNSPCs exhibited a neuroprotective effect *in vitro* against glutamate-induced excitotoxicity via paracrine mechanisms. Taken together, our results provide evidence that hNSPC transplantation into the LV has potential therapeutic effects for suppressing seizures in a TLE model.

Next, we generated GAL-hNSPCs using adenoviral vector to assess the therapeutic effects of combined hNSPC and gene therapy in the rat lithium-

pilocarpine model of TLE. After SRMS confirmation, epileptic rats were injected with vehicle, GFP-hNSPCs, or GAL-hNSPCs into the CA3 regions of the bilateral hippocampi. Grafted GFP-hNSPCs or GAL-hNSPCs migrated from the injection site and dispersed throughout the hippocampus, and differentiated into TUJ1-, GFAP-, OLIG2-, and GABA-expressing cells. GFP-hNSPC transplantation significantly reduced the frequency and duration of SRMS at 3 months post-transplants, while GAL-hNSPC transplantation significantly reduced SRMS through all the time periods for 3 months following implantation.

Intrahippocampal transplantation of GFP-hNSPCs or GAL-hNSPCs resulted in the addition of donor-derived GABA-expressing cells into the hippocampus, considerable preservation of the pyramidal neurons of the hippocampus, and a significant reduction of MFS, highlighting the beneficial effects of these cells in this model. In addition, GAL-hNSPC-transplanted group exhibited the recovery of emotional deficit and reversal of decreased neurogenesis of the hippocampus of epileptic rats which were not observed in GFP-hNSPC-transplanted group and presented seizure suppression and extensive neuroprotection more significantly as compared to GFP-hNSPC-transplanted group. Thus, this study provides the first evidence that galanin-secreting hNSPC transplantation into adult epileptic rat brain exerts therapeutic effects against SRMS and emotional deficit and for increasing neurogenesis and neuroprotection in the hippocampus of the lithium-pilocarpine induced TLE model, representing a novel combined stem cell and gene therapy in severely epileptic rats.

REFERENCES

1. Banerjee PN, Filippi D, Allen Hauser W. The descriptive epidemiology of epilepsy—A review. Epilepsy Research 2009;85:31-45.
2. Fisher PD, Sperber EF, Moshé SL. Hippocampal sclerosis revisited. Brain and Development 1998;20:563-73.
3. Morimoto K, Fahnestock M, Racine RJ. Kindling and status epilepticus models of epilepsy: rewiring the brain. Progress in Neurobiology 2004;73:1-60.
4. André V, Marescaux C, Nehlig A, Fritschy JM. Alterations of hippocampal GABAergic system contribute to development of spontaneous recurrent seizures in the rat lithium-pilocarpine model of temporal lobe epilepsy. Hippocampus 2001;11:452-68.
5. Detour J, Schroeder H, Desor D, Nehlig A. A 5-Month Period of Epilepsy Impairs Spatial Memory, Decreases Anxiety, but Spares Object Recognition in the Lithium-pilocarpine Model in Adult Rats. Epilepsia 2005;46:499-508.
6. Rossi AR, Angelo MF, Villarreal A, Lukin J, Ramos AJ. Gabapentin administration reduces reactive gliosis and neurodegeneration after pilocarpine-induced status epilepticus. PLoS ONE 2013;8:e78516.
7. Chakir A, Fabene PF, Ouazzani R, Bentivoglio M. Drug resistance and hippocampal damage after delayed treatment of pilocarpine-induced epilepsy in the rat. Brain Research Bulletin 2006;71:127-38.
8. Mello LE, Cavalheiro EA, Tan AM, Kupfer WR, Pretorius JK, Babb TL, et al. Circuit mechanisms of seizures in the pilocarpine model of chronic epilepsy: cell loss and mossy fiber sprouting. Epilepsia 1993;34:985-95.
9. Hattiangady B, Rao MS, Shetty AK. Chronic temporal lobe epilepsy is associated with severely declined dentate neurogenesis in the adult hippocampus. Neurobiology of Disease 2004;17:473-90.

10. Waldau B, Hattiangady B, Kuruba R, Shetty AK. Medial Ganglionic Eminence-Derived Neural Stem Cell Grafts Ease Spontaneous Seizures and Restore GDNF Expression in a Rat Model of Chronic Temporal Lobe Epilepsy. STEM CELLS 2010;28:1153-64.
11. Ravizza T, Gagliardi B, Noé F, Boer K, Aronica E, Vezzani A. Innate and adaptive immunity during epileptogenesis and spontaneous seizures: Evidence from experimental models and human temporal lobe epilepsy. Neurobiology of Disease 2008;29:142-60.
12. Heller AC, Padilla RV, Mamelak AN. Complications of epilepsy surgery in the first 8 years after neurosurgical training. Surgical Neurology 2009;71:631-7.
13. Roper SN, Steindler DA. Stem cells as a potential therapy for epilepsy. Experimental Neurology 2013;244:59-66.
14. Sørensen AT, Kokaia M. Novel approaches to epilepsy treatment. Epilepsia 2013;54:1-10.
15. Löscher W, Gernert M, Heinemann U. Cell and gene therapies in epilepsy – promising avenues or blind alleys? Trends in Neurosciences 2008;31:62-73.
16. Maisano X, Litvina E, Tagliatela S, Aaron GB, Grabel LB, Naegele JR. Differentiation and Functional Incorporation of Embryonic Stem Cell-Derived GABAergic Interneurons in the Dentate Gyrus of Mice with Temporal Lobe Epilepsy. The Journal of Neuroscience 2012;32:46-61.
17. Shindo A, Nakamura T, Matsumoto Y, Kawai N, Okano H, Nagao S, et al. Seizure Suppression in Amygdala-Kindled Mice by Transplantation of Neural Stem/Progenitor Cells Derived From Mouse Embryonic Stem Cells. Neurologia medico-chirurgica 2010;50:98-106.
18. Carpentino JE, Hartman NW, Grabel LB, Naegele JR. Region-specific differentiation of embryonic stem cell-derived neural progenitor transplants into the adult mouse hippocampus following seizures. Journal

of Neuroscience Research 2008;86:512-24.

19. Rüschenschmidt C, Koch PG, Brüstle O, Beck H. Functional Properties of ES Cell–Derived Neurons Engrafted into the Hippocampus of Adult Normal and Chronically Epileptic Rats. Epilepsia 2005;46:174-83.
20. Hattiangady B, Rao MS, Shetty AK. Grafting of striatal precursor cells into hippocampus shortly after status epilepticus restrains chronic temporal lobe epilepsy. Experimental Neurology 2008;212:468-81.
21. Zanirati G, Azevedo PN, Marinowic DR, Rodrigues F, de Oliveira Dias AC, Venturin GT, et al. Transplantation of Bone Marrow Mononuclear Cells Modulates Hippocampal Expression of Growth Factors in Chronically Epileptic Animals. CNS Neuroscience & Therapeutics 2015:n/a-n/a.
22. Costa-Ferro ZSM, Souza BSF, Leal MMT, Kaneto CM, Azevedo CM, da Silva IC, et al. Transplantation of bone marrow mononuclear cells decreases seizure incidence, mitigates neuronal loss and modulates pro-inflammatory cytokine production in epileptic rats. Neurobiology of Disease 2012;46:302-13.
23. Hunt RF, Girskis KM, Rubenstein JL, Alvarez-Buylla A, Baraban SC. GABA progenitors grafted into the adult epileptic brain control seizures and abnormal behavior. Nat Neurosci 2013;16:692-7.
24. Baraban SC, Southwell DG, Estrada RC, Jones DL, Sebe JY, Alfaro-Cervello C, et al. Reduction of seizures by transplantation of cortical GABAergic interneuron precursors into Kv1.1 mutant mice. Proceedings of the National Academy of Sciences 2009;106:15472-7.
25. Chu K, Kim M, Jung K-H, Jeon D, Lee S-T, Kim J, et al. Human neural stem cell transplantation reduces spontaneous recurrent seizures following pilocarpine-induced status epilepticus in adult rats. Brain Research 2004;1023:213-21.
26. Kim T-G, Yao R, Monnell T, Cho J-H, Vasudevan A, Koh A, et al.

Efficient Specification of Interneurons from Human Pluripotent Stem Cells by Dorsoventral and Rostrocaudal Modulation. STEM CELLS 2014;32:1789-804.

27. Kim H-T, Kim I-S, Lee I-S, Lee J-P, Snyder EY, In Park K. Human neurospheres derived from the fetal central nervous system are regionally and temporally specified but are not committed. Experimental Neurology 2006;199:222-35.
28. Jin K, Sun Y, Xie L, Mao XO, Childs J, Peel A, et al. Comparison of ischemia-directed migration of neural precursor cells after intrastriatal, intraventricular, or intravenous transplantation in the rat. Neurobiology of disease 2005;18:366-74.
29. Park KI, Himes BT, Stieg PE, Tessler A, Fischer I, Snyder EY. Neural stem cells may be uniquely suited for combined gene therapy and cell replacement: Evidence from engraftment of Neurotrophin-3-expressing stem cells in hypoxic–ischemic brain injury. Experimental Neurology 2006;199:179-90.
30. Park KI, Teng YD, Snyder EY. The injured brain interacts reciprocally with neural stem cells supported by scaffolds to reconstitute lost tissue. Nat Biotech 2002;20:1111-7.
31. Tamaki SJ, Jacobs Y, Dohse M, Capela A, Cooper JD, Reitsma M, et al. Neuroprotection of host cells by human central nervous system stem cells in a mouse model of infantile neuronal ceroid lipofuscinosis. Cell stem cell 2009;5:310-9.
32. Meng X, Shen J, Ohashi T, Maeda H, Kim SU, Eto Y. Brain transplantation of genetically engineered human neural stem cells globally corrects brain lesions in the mucopolysaccharidosis type VII mouse. Journal of neuroscience research 2003;74:266-77.
33. Inostroza M, Cid E, Brotons Mas J, Gal B, Aivar P, Uzcategui YG, et al. Hippocampal-dependent spatial memory in the water maze is preserved

in an experimental model of temporal lobe epilepsy in rats. PLoS ONE 2011;6:e22372.

34. Weinberg MS, McCown TJ. Current prospects and challenges for epilepsy gene therapy. Experimental Neurology 2013;244:27-35.
35. Haberman RP, Samulski RJ, McCown TJ. Attenuation of seizures and neuronal death by adeno-associated virus vector galanin expression and secretion. Nature medicine 2003;9:1076-80.
36. Nikitidou L, Torp M, Fjord-Larsen L, Kusk P, Wahlberg LU, Kokaia M. Encapsulated galanin-producing cells attenuate focal epileptic seizures in the hippocampus. Epilepsia 2014;55:167-74.
37. Kanter-Schlifke I, Toft Sørensen A, Ledri M, Kuteeva E, Hökfelt T, Kokaia M. Galanin gene transfer curtails generalized seizures in kindled rats without altering hippocampal synaptic plasticity. Neuroscience 2007;150:984-92.
38. Mazarati A, Lu X. Regulation of limbic status epilepticus by hippocampal galanin type 1 and type 2 receptors. Neuropeptides 2005;39:277-80.
39. Mazarati AM, Liu H, Soomets U, Sankar R, Shin D, Katsumori H, et al. Galanin Modulation of Seizures and Seizure Modulation of Hippocampal Galanin in Animal Models of Status Epilepticus. The Journal of Neuroscience 1998;18:10070-7.
40. Mazarati AM. Galanin and galanin receptors in epilepsy. Neuropeptides 2004;38:331-43.
41. Zini S, Roisin MP, Langel U, Bartfai T, Ben Ari Y. Galanin reduces release of endogenous excitatory amino acids in the rat hippocampus. European journal of pharmacology 1993;245:1-7.
42. Zini S, Roisin MP, Armengaud C, Ben Ari Y. Effect of potassium channel modulators on the release of glutamate induced by ischaemic-like conditions in rat hippocampal slices. Neuroscience Letters 1993;153:202-

5.
43. Palazzi E, Felinska S, Zambelli M, Fisone G, Bartfai T, Consolo S. Galanin Reduces Carbachol Stimulation of Phosphoinositide Turnover in Rat Ventral Hippocampus by Lowering Ca2+ Influx Through Voltage-Sensitive Ca2+ Channels. Journal of Neurochemistry 1991;56:739-47.
44. McCown TJ. Adeno-associated Virus-Mediated Expression and Constitutive Secretion of Galanin Suppresses Limbic Seizure Activity in Vivo. Mol Ther 2006;14:63-8.
45. Lin E-JD, Richichi C, Young D, Baer K, Vezzani A, During MJ. Recombinant AAV-mediated expression of galanin in rat hippocampus suppresses seizure development. European Journal of Neuroscience 2003;18:2087-92.
46. Park S, Kim H-T, Yun S, Kim I-S, Lee J, Lee I-S, et al. Growth factor-expressing human neural progenitor cell grafts protect motor neurons but do not ameliorate motor performance and survival in ALS mice. Exp Mol Med 2009;41:487-500.
47. Racine RJ. Modification of seizure activity by electrical stimulation: II. Motor seizure. Electroencephalography and Clinical Neurophysiology 1972;32:281-94.
48. Zhang T, Cho H, Lee S, Lee J-H, Choi S, Ryu V, et al. Impairments in water maze learning of aged rats that received dextromethorphan repeatedly during adolescent period. Psychopharmacology 2007;191:171-9.
49. Bolanos AR, Sarkisian M, Yang Y, Hori A, Helmers SL, Mikati M, et al. Comparison of valproate and phenobarbital treatment after status epilepticus in rats. Neurology 1998;51:41-8.
50. Cilio MR, Bolanos AR, Liu Z, Schmid R, Yang Y, Stafstrom CE, et al. Anticonvulsant action and long-term effects of gabapentin in the immature brain. Neuropharmacology 2001;40:139-47.

51. van Vliet EA, Aronica E, Tolner EA, Lopes da Silva FH, Gorter JA. Progression of temporal lobe epilepsy in the rat is associated with immunocytochemical changes in inhibitory interneurons in specific regions of the hippocampal formation. Experimental Neurology 2004;187:367-79.
52. Dubé C, Boyet S, Marescaux C, Nehlig A. Relationship between Neuronal Loss and Interictal Glucose Metabolism during the Chronic Phase of the Lithium-Pilocarpine Model of Epilepsy in the Immature and Adult Rat. Experimental Neurology 2001;167:227-41.
53. Dykstra CM, Ratnam M, Gurd JW. Neuroprotection after status epilepticus by targeting protein interactions with postsynaptic density protein 95. Journal of neuropathology and experimental neurology 2009;68:823-31.
54. Jiao Y, Nadler JV. Stereological analysis of GluR2-immunoreactive hilar neurons in the pilocarpine model of temporal lobe epilepsy: Correlation of cell loss with mossy fiber sprouting. Experimental Neurology 2007;205:569-82.
55. Bausch SB, McNamara JO. Contributions of Mossy Fiber and CA1 Pyramidal Cell Sprouting to Dentate Granule Cell Hyperexcitability in Kainic Acid–Treated Hippocampal Slice Cultures; 2004.
56. Tian F, Zeng C, Guo T, Chen Y, Chen J, Ma Y, et al. Mossy fiber sprouting, hippocampal damage and spontaneous recurrent seizures in pentylenetetrazole kindling rat model. Acta neurologica belgica 2009;109:298-304.
57. Pun RY, Rolle IJ, Lasarge CL, Hosford BE, Rosen JM, Uhl JD, et al. Excessive activation of mTOR in postnatally generated granule cells is sufficient to cause epilepsy. Neuron 2012;75:1022-34.
58. Paxinos G, Watson C. The rat brain in stereotaxic coordinates. London :: Academic Press; 2009.

59. Farioli-Vecchioli S, Micheli L, Saraulli D, Ceccarelli M, Cannas S, Scardigli R, et al. BTG1 is required to maintain the pool of stem and progenitor cells of dentate gyrus and subventricular zone. Frontiers in Neuroscience 2012;6.
60. Spandidos A, Wang X, Wang H, Seed B. PrimerBank: a resource of human and mouse PCR primer pairs for gene expression detection and quantification. Nucleic Acids Research 2010;38:D792-D9.
61. Meberg PJ, Miller MW. Culturing Hippocampal and Cortical Neurons. Methods in Cell Biology: Academic Press; 2003. p.111-27.
62. Hockfield S, McKay RD. Identification of major cell classes in the developing mammalian nervous system. The Journal of neuroscience 1985;5:3310-28.
63. Choi BH, Lapham LW. Radial glia in the human fetal cerebrum: A combined golgi, immunofluorescent and electron microscopic study. Brain Research 1978;148:295-311.
64. Dahl D, Rueger DC, Bignami A. Vimentin, the 57000 molecular weight protein of fibroblast filaments, is the major cytoskeletal component in immature glia. European Journal of Cell Biology 1981;24:191-6.
65. Levitt P, Cooper ML, Rakic P. Early divergence and changing proportions of neuronal and glial precursor cells in the primate cerebral ventricular zone. Developmental Biology 1983;96:472-84.
66. Choi BH. Glial fibrillary acidic protein in radial glia of early human fetal cerebrum: A light and electron microscopic immunoperoxidase study. Journal of Neuropathology and Experimental Neurology 1986;45:408-18.
67. Alvarez-Buylla A, García-Verdugo JM, Tramontin AD. A unified hypothesis on the lineage of neural stem cells. Nature Reviews Neuroscience 2001;2:287-93.
68. Zecevic N. Specific characteristic of radial glia in the human fetal telencephalon. GLIA 2004;48:27-35.

69. Malatesta P, Hack MA, Hartfuss E, Kettenmann H, Klinkert W, Kirchhoff F, et al. Neuronal or Glial Progeny: Regional Differences in Radial Glia Fate. Neuron 2003;37:751-64.
70. Hartfuss E, Galli R, Heins N, Götz M. Characterization of CNS Precursor Subtypes and Radial Glia. Developmental Biology 2001;229:15-30.
71. Pevny L, Rao MS. The stem-cell menagerie. Trends in Neurosciences 2003;26:351-9.
72. Uchida N, Buck DW, He D, Reitsma MJ, Masek M, Phan TV, et al. Direct isolation of human central nervous system stem cells. Proceedings of the National Academy of Sciences 2000;97:14720-5.
73. Flax JD, Aurora S, Yang C, Simonin C, Wills AM, Billinghurst LL, et al. Engraftable human neural stem cells respond to development cues, replace neurons, and express foreign genes. Nat Biotech 1998;16:1033-9.
74. Keyoung HM, Roy NS, Benraiss A, Louissaint A, Suzuki A, Hashimoto M, et al. High-yield selection and extraction of two promoter-defined phenotypes of neural stem cells from the fetal human brain. Nat Biotech 2001;19:843-50.
75. Conti L, Cattaneo E. Neural stem cell systems: physiological players or in vitro entities? Nat Rev Neurosci 2010;11:176-87.
76. Frisch C, Kudin AP, Elger CE, Kunz WS, Helmstaedter C. Amelioration of water maze performance deficits by topiramate applied during pilocarpine-induced status epilepticus is negatively dose-dependent. Epilepsy Research 2007;73:173-80.
77. Nishimura T, Imai H, Minabe Y, Sawa A, Kato N. Beneficial effects of FK506 for experimental temporal lobe epilepsy. Neuroscience research 2006;56:386-90.
78. Dinocourt C, Petanjek Z, Freund TF, Ben Ari Y, Esclapez M. Loss of interneurons innervating pyramidal cell dendrites and axon initial segments in the CA1 region of the hippocampus following pilocarpine-

induced seizures. Journal of comparative neurology 2003;459:407-25.
79. Maglóczky Z. Sprouting in human temporal lobe epilepsy: Excitatory pathways and axons of interneurons. Epilepsy Research 2010;89:52-9.
80. Sharma AK, Reams RY, Jordan WH, Miller MA, Thacker HL, Snyder PW. Mesial Temporal Lobe Epilepsy: Pathogenesis, Induced Rodent Models and Lesions. Toxicologic Pathology 2007;35:984-99.
81. Clasadonte J, Dong J, Hines DJ, Haydon PG. Astrocyte control of synaptic NMDA receptors contributes to the progressive development of temporal lobe epilepsy. Proceedings of the National Academy of Sciences of the United States of America 2013;110:17540-5.
82. Ortinski PI, Dong J, Mungenast A, Yue C, Takano H, Watson DJ, et al. Selective induction of astrocytic gliosis generates deficits in neuronal inhibition. Nature neuroscience 2010;13:584-91.
83. Kanter Schlifke I, Georgievska B, Kirik D, Kokaia M. Seizure suppression by GDNF gene therapy in animal models of epilepsy. Molecular therapy 2007;15:1106-13.
84. Kanter-Schlifke I, Fjord-Larsen L, Kusk P, Ängehagen M, Wahlberg L, Kokaia M. GDNF released from encapsulated cells suppresses seizure activity in the epileptic hippocampus. Experimental Neurology 2009;216:413-9.
85. Drago D, Cossetti C, Iraci N, Gaude E, Musco G, Bachi A, et al. The stem cell secretome and its role in brain repair. Biochimie 2013;95:2271-85.
86. Almeida RD, Manadas BJ, Melo CV, Gomes JR, Mendes CS, Graos MM, et al. Neuroprotection by BDNF against glutamate-induced apoptotic cell death is mediated by ERK and PI3-kinase pathways. Cell Death Differ 2005;12:1329-43.
87. Jin K, LaFevre-Bernt M, Sun Y, Chen S, Gafni J, Crippen D, et al. FGF-2 promotes neurogenesis and neuroprotection and prolongs survival in a

transgenic mouse model of Huntington's disease. Proceedings of the National Academy of Sciences of the United States of America 2005;102:18189-94.

88. Sypecka J, Sarnowska A. The Neuroprotective Effect Exerted by Oligodendroglial Progenitors on Ischemically Impaired Hippocampal Cells. Molecular Neurobiology 2014;49:685-701.
89. Taoufik E, Petit E, Divoux D, Tseveleki V, Mengozzi M, Roberts ML, et al. TNF receptor I sensitizes neurons to erythropoietin- and VEGF-mediated neuroprotection after ischemic and excitotoxic injury. Proceedings of the National Academy of Sciences 2008;105:6185-90.
90. Yoo Y-M, Lee C-J, Lee U, Kim Y-J. Neuroprotection of adenoviral-vector-mediated GDNF expression against kainic-acid-induced excitotoxicity in the rat hippocampus. Experimental Neurology 2006;200:407-17.
91. De Simoni MG, Perego C, Ravizza T, Moneta D, Conti M, Marchesi F, et al. Inflammatory cytokines and related genes are induced in the rat hippocampus by limbic status epilepticus. European Journal of Neuroscience 2000;12:2623-33.
92. Jung K-H, Chu K, Lee S-T, Kim J, Sinn D-I, Kim J-M, et al. Cyclooxygenase-2 inhibitor, celecoxib, inhibits the altered hippocampal neurogenesis with attenuation of spontaneous recurrent seizures following pilocarpine-induced status epilepticus. Neurobiology of Disease 2006;23:237-46.
93. Marchi N, Fan Q, Ghosh C, Fazio V, Bertolini F, Betto G, et al. Antagonism of peripheral inflammation reduces the severity of status epilepticus. Neurobiology of Disease 2009;33:171-81.
94. Maroso M, Balosso S, Ravizza T, Iori V, Wright C, French J, et al. Interleukin-1β Biosynthesis Inhibition Reduces Acute Seizures and Drug Resistant Chronic Epileptic Activity in Mice. Neurotherapeutics

2011;8:304-15.

95. Maroso M, Balosso S, Ravizza T, Liu J, Aronica E, Iyer AM, et al. Toll-like receptor 4 and high-mobility group box-1 are involved in ictogenesis and can be targeted to reduce seizures. Nat Med 2010;16:413-9.
96. Polascheck N, Bankstahl M, Löscher W. The COX-2 inhibitor parecoxib is neuroprotective but not antiepileptogenic in the pilocarpine model of temporal lobe epilepsy. Experimental Neurology 2010;224:219-33.
97. Agasse F, Xapelli S, Coronas V, Christiansen SH, Rosa AI, Sardá Arroyo L, et al. Galanin promotes neuronal differentiation in murine subventricular zone cell cultures. Stem cells and development 2013;22:1693-708.
98. Dos Santos JG, Longo BM, Blanco MM, Menezes de Oliveira MG, Mello LE. Behavioral changes resulting from the administration of cycloheximide in the pilocarpine model of epilepsy. Brain research 2005;1066:37-48.
99. Abbosh C, Lawkowski A, Zaben M, Gray W. GalR2/3 mediates proliferative and trophic effects of galanin on postnatal hippocampal precursors. Journal of Neurochemistry 2011;117:425-36.
100. Maglóczky Z, Freund TF. Impaired and repaired inhibitory circuits in the epileptic human hippocampus. Trends in Neurosciences 2005;28:334-40.
101. Cossart R, Dinocourt C, Hirsch JC, Merchan Perez A, De Felipe J, Ben Ari Y, et al. Dendritic but not somatic GABAergic inhibition is decreased in experimental epilepsy. Nature neuroscience 2001;4:52-62.
102. Kobayashi M, Buckmaster PS. Reduced inhibition of dentate granule cells in a model of temporal lobe epilepsy. The Journal of neuroscience 2003;23:2440-52.
103. Celio MR. Calbindin D-28k and parvalbumin in the rat nervous system. Neuroscience 1990;35:375-475.
104. Tanabe K, Matsushima-Nishiwaki R, Iida M, Kozawa O, Iida H.

Involvement of phosphatidylinositol 3-kinase/Akt on basic fibroblast growth factor-induced glial cell line-derived neurotrophic factor release from rat glioma cells. Brain Research 2012;1463:21-9.

105. Shin SY, Song H, Kim CG, Choi Y-K, Lee KS, Lee S-J, et al. Egr-1 Is Necessary for Fibroblast Growth Factor-2-induced Transcriptional Activation of the Glial Cell Line-derived Neurotrophic Factor in Murine Astrocytes. Journal of Biological Chemistry 2009;284:30583-93.
106. Burns K, Martinon F, Tschopp J. New insights into the mechanism of IL-1beta maturation. Current opinion in immunology 2003;15:26-30.
107. Vezzani A, Moneta D, Conti M, Richichi C, Ravizza T, De Luigi A, et al. Powerful anticonvulsant action of IL-1 receptor antagonist on intracerebral injection and astrocytic overexpression in mice. Proceedings of the National Academy of Sciences 2000;97:11534-9.
108. Corti S, Locatelli F, Papadimitriou D, Del Bo R, Nizzardo M, Nardini M, et al. Neural stem cells LewisX + CXCR4 + modify disease progression in an amyotrophic lateral sclerosis model; 2007.
109. Ourednik J, Ourednik V, Lynch WP, Schachner M, Snyder EY. Neural stem cells display an inherent mechanism for rescuing dysfunctional neurons. Nat Biotech 2002;20:1103-10.
110. Ryu JK, Kim J, Cho SJ, Hatori K, Nagai A, Choi HB, et al. Proactive transplantation of human neural stem cells prevents degeneration of striatal neurons in a rat model of Huntington disease. Neurobiology of Disease 2004;16:68-77.
111. Yasuhara T, Matsukawa N, Hara K, Yu G, Xu L, Maki M, et al. Transplantation of Human Neural Stem Cells Exerts Neuroprotection in a Rat Model of Parkinson's Disease. The Journal of Neuroscience 2006;26:12497-511.
112. Aguado T, Monory K, Palazuelos J, Stella N, Cravatt B, Lutz B, et al. The endocannabinoid system drives neural progenitor proliferation. The

FASEB Journal 2005.

113. Butti E, Bacigaluppi M, Rossi S, Cambiaghi M, Bari M, Cebrian Silla A, et al. Subventricular zone neural progenitors protect striatal neurons from glutamatergic excitotoxicity. Brain 2012;135:3320-35.
114. Molina Holgado F, Pinteaux E, Moore JD, Molina Holgado E, Guaza C, Gibson RM, et al. Endogenous interleukin-1 receptor antagonist mediates anti-inflammatory and neuroprotective actions of cannabinoids in neurons and glia. The Journal of neuroscience 2003;23:6470-4.
115. Maglóczky Z, Freund TF. Impaired and repaired inhibitory circuits in the epileptic human hippocampus. Trends in neurosciences 2005;28:334-40.
116. Sharma AK, Reams RY, Jordan WH, Miller MA, Thacker HL, Snyder PW. Mesial temporal lobe epilepsy: pathogenesis, induced rodent models and lesions. Toxicologic pathology 2007;35:984-99.
117. Shetty AK, Turner DA. Glutamic acid decarboxylase-67-positive hippocampal interneurons undergo a permanent reduction in number following kainic acid-induced degeneration of ca3 pyramidal neurons. Experimental neurology 2001;169:276-97.
118. Elliott-Hunt CR, Marsh B, Bacon A, Pope R, Vanderplank P, Wynick D. Galanin acts as a neuroprotective factor to the hippocampus. Proceedings of the National Academy of Sciences of the United States of America 2004;101:5105-10.
119. Xie C, Sun J, Qiao W, Lu D, Wei L, Na M, et al. Administration of Simvastatin after Kainic Acid-Induced Status Epilepticus Restrains Chronic Temporal Lobe Epilepsy. PLoS ONE 2011;6:e24966.
120. Shetty AK, Turner DA. Fetal Hippocampal Cells Grafted to Kainate-Lesioned CA3 Region of Adult Hippocampus Suppress Aberrant Supragranular Sprouting of Host Mossy Fibers. Experimental Neurology 1997;143:231-45.
121. Rao MS, Hattiangady B, Shetty AK. Fetal hippocampal CA3 cell grafts

enriched with FGF-2 and BDNF exhibit robust long-term survival and integration and suppress aberrant mossy fiber sprouting in the injured middle-aged hippocampus. Neurobiology of Disease 2006;21:276-90.

ABSTRACT (IN KOREAN)

측두엽 간질 동물 모델에서 인간 신경줄기/전구세포를 이용한 세포 및 유전자 치료

<지도교수 박국인>

연세대학교 대학원 의과학과

이혜진

간질(epilepsy)은 전 인구의 약 1%가 이환 되어 높은 유병율을 보이는 만성 신경계질환으로, 간질 환자의 약 40%가 측두엽 간질(temporal lobe epilepsy) 환자 이다. 측두엽 간질 환자 및 동물모델에서 가장 일반적으로 관찰되는 병리소견은 해마경화(hippocampal sclerosis)인데, 해마뉴런의 손실과 태상 섬유 발아(mossy fiber sprouting) 등이 특징 소견이다.

신경줄기/전구세포 (neural stem/progenitor cells; NSPCs)는 신경계 이식을 통하여 치료적으로 유용한 물질을 직접적이고 안정적으로 분비하게 할뿐만 아니라, 기능부전을 보이는 신경세포를 대체하고, 손상된 신경망을 재건하여 중추신경계를 재생케 하는 가능성을 보인다.

본 연구는 측두엽 간질 모델에서 인간 신경줄기/전구세포 이식의 치료적 유용성을 조사하였는데, 리튬-필로카르핀 유발 측두엽 간질 흰쥐 모델을 사용하였고, 인간 신경줄기/전구세포는 임신 13주에 자연 유산된 태아의 종뇌에서 분리·배양하였다. 자발적 반복 운동성

발작이 관찰된 측두엽 간질 흰쥐의 측 내실 (lateral ventricles)에 인간 신경줄기/전구세포를 이식하고 3개월 후 분석한 결과, 공여세포는 모델 쥐 뇌의 다양한 부위에 걸쳐 광범위하게 이주 및 생착함을 보였고, 일부 공여세포는 신경원세포, 희소돌기아교세포 전구세포 및 성상교세포로 분화하였지만 대부분의 공여세포는 주로 미분화 상태로 존재하였다. 인간 신경줄기/전구세포를 이식한 실험군은 식염수를 주사한 대조군과 비교하여 통계적으로 유의하게 자발성 반복 운동성 발작의 빈도와 지속 시간이 감소됨을 보였고, 실험군의 해마에서 뉴런 손실 감소, 숙주 성상교세포에서 항경련성 신경영양인자인 glial cell-derived neurotrophic factor (GDNF) 발현 및 항염증 싸이토카인 증가를 유도하였다. 또한, 인간 신경줄기/전구세포 유래 conditioned medium은 시험관 내에서 글루탐산 흥분 독성에 의한 해마 신경원세포 사멸을 억제함을 보였다. 따라서 난치성 만성 신경계 질환인 측두엽 간질 동물 모델에서 인간 신경줄기/전구세포 이식이 유용한 세포치료법으로 사용될 수 있음을 제시하였다.

난치성 간질 모델에서 줄기세포 치료뿐만 아니라 세포유전자 치료의 치료적 유용성을 조사하기 위하여, 먼저 항경련성 신경펩타이드인 galanin 유전자를 클로닝하여 아데노바이러스 (adenovirus) 벡터를 제작하고, 인간 신경줄기/전구세포에 감염시켜 galanin 분비 인간 신경줄기/전구세포 (GAL-hNSPCs)를 확립하였다. GAL-hNSPCs와 녹색형광단백질을 발현하는 인간 신경줄기/전구세포 (green fluorescent protein [GFP]-hNSPC)를 자발성 반복 운동성 발작이 관찰된 측두엽 간질 모델 흰쥐의 해마에 이식하고 3개월 후 분석한 결과, 두 그룹 모두 이식세포가 간질 동물의 해마에서 광범위하게 이주 및 생착함을 보였고,

신경원세포, 희소돌기아교세포 전구세포, 성상교세포 및 GABA 발현 세포로 분화함을 보였다. 식염수를 이식한 대조군에 비해, GFP-hNSPCs를 이식한 실험군은 SRMS의 빈도와 지속 시간이 이식 후 한 달째부터 감소하여 세 달째에 통계적으로 유의하게 감소함을 보인 반면, GAL-hNSPCs를 이식한 실험군은 이식 한 달 후부터 세 달째까지 모두 통계적으로 유의하게 SRMS가 감소함을 보였다. 또한 GAL-hNSPCs를 이식한 실험군에서는 비정상적으로 낮은 수준의 불안 정서가 정상 수준으로 회복됨을 보였다. 또한 GFP-hNSPCs 또는 GAL-hNSPCs를 이식한 실험군의 해마에서 뉴런 손실의 감소, 태상 섬유 발아 억제 및 숙주 성상교세포에서 GDNF 발현 유도가 관찰되었으나, GFP-hNSPCs를 이식한 실험군과 비교하여 GAL-hNSPCs를 이식한 실험군에서 뉴런 보호 효과가 더욱 향상됨을 보였고, 만성 간질 해마에서 주로 나타나는 신경세포생성 (neurogenesis)의 감소가 회복됨을 관찰하였다. 따라서 측두엽 간질 동물 모델에서 galanin 분비 인간 신경줄기/전구세포의 이식은 간질 발작을 감소시키고, 불안 정서 장애를 회복시키며, 해마에서 신경보호 및 신경생성을 촉진시키는 새로운 줄기세포 매개 세포유전자치료법 임을 제시하였다.

핵심되는 말 : 측두엽 간질, 인간 신경줄기/전구세포, 측두엽 간질 모델, 세포이식, 세포 치료, 유전자 치료, 갈라닌